Diploma Thesis

Assessment of the water proton diffusivity in the post mortem brain

Michael Steiner

Institute of Medical Engineering
Graz University of Technologie
Head: Rudolf Stollberger, PhD

Adviser:

Stefan Ropele, PhD
Rudolf Stollberger, PhD

Graz, February 2013

Abstract

Magnet resonance tomography makes it possible to show functional processes in the body without using contrast agents. The used technique, the diffusion imaging, makes it possible to measure the molecular processes of the protons and to research the self diffusion of water. The functional activities of the self diffusion remains after death and therefore it is interesting in a forensically point of view to analyze the changes. The assessment of the data sets was done with an echo planar single-shot sequence. Temperature is one of the basic parameters of diffusion. Many research theses investigated in diffusion dependent thermometry, which were the background for the realized models. In our case, the thermometry had to be done in corpses, which lead to special conditions. To assess the temperature two models were carried out. The first model will represent the accepted opinion that the liquor cerebrospinal is similar to water and therefore the diffusion coefficient of water will be also similar. The second model represents a more critical aspect. It is known, that there will be cells in the subarachnoid space due to autolysis after death. Those cells lead to an attenuation of the diffusion coefficients and therefore to an attenuation of the assessed temperature. The reasons for these changes in the diffusion coefficient will be discussed more precisely within the theses. To recognize the influences of death on the tissue it is important to separate the effects of temperature and post mortem delay. The results show, that an accurate separation of the influences is not possible.

Keywords: nuclear magnetic resonance, magnetic resonance thermometry; diffusion imaging; post mortem imaging;

Kurzfassung

Mittels Magnetresonanztomographie ist es möglich die funktionellen Abläufe im Körper ohne Kontrastmittel darzustellen. Die dazu benutzte Technik, die Diffusionsbildgebung, ermöglicht es die molekularen Prozesse der Protonen zu messen und die Selbstdiffusion von Wasser zu ergründen. Da diese funktionellen Abläufe der Selbstdiffusion nach dem Tode weiterhin aktiv sind, ist es aus forensischer Sicht interessant die Unterschiede zu untersuchen. Die Erfassung der diffusionsbezogenen Daten wurde mit einer Echoplanaren Single-Shot Sequenz durchgeführt. Ein grundlegenderer Parameter der Diffusion ist die Temperatur. Viele Forschungsarbeiten haben sich mit der diffusionsabhängigen Thermometrie beschäftigt, welche hier als Vorlage für die durchgenommen Methoden dienten. Da die Thermometrie in unserem Fall bei Leichen durchgeführt wird, ergeben sich spezielle Zustände. Für die Bestimmung der Temperatur werden zwei Modelle genauer betrachtet. Das eine Modell vertritt die weitläufige Annahme, dass sich der Liquor cerebrospinalis mit Wasser ähnelt und daher die Diffusionskoeffizienten nicht wesentlich unterscheiden. Das zweite Modell vertritt einen kritischeren Standpunkt. Es ist bekannt, dass sich nach dem Tode Autolyse bedingt Zellen in den Liquor-Raum gelangen. Diese Zellen führen zu einer Absenkung des Diffusionskoeffizienten und daraus zu einer Abweichung der Temperaturabschätzung. Die Gründe der Absenkung des Diffusionskoeffizienten werden innerhalb dieser Arbeit genauer diskutiert. Um die genauen Einflüsse des Todes auf das Gewebe zu erkennen ist es wichtig, die Einflüsse von Zeit und Temperatur zu trennen. Die Resultate zeigten, dass eine genaue Trennung der Einflüsse nicht eindeutig möglich ist.

Schlagwörter: Magnetresonant; Magnetresonanz Thermometrie; Diffusionsbildgebung. Postmortale Bildgebung;

Contents

1 Introduction

1.1 Background

Magnetic resonance imaging (MRI) is one of the most versatile non invasive imaging method which is used in medicine. Identifying objects or actions usually needs more than one examination technique. Most of these methods are based on combined acquisition techniques using multiple sources of sensory inputs. Typical observation factors are sounds or contrast agents based imaging techniques. Many contrast agents are radioactive. Using these lead to a nonessential contamination of the body. MRI can be used for functional imaging without using contrast agents. MRI is based on the molecular properties of water protons which can be modulated by the microscopic tissue compartments. For example blood flow may be detected by using the signal changes due to phase encoded gradient fields.

An important clinical application of magnet resonance imaging is diffusion imaging. The Brownian motion of water is used to get information of the self-diffusion within the cells. Due to the restriction of water diffusion on the intracellular structures and cellular membranes it is possible to get macroscopic information of the cells. The favorable characteristics of brain tissue are the reason why diffusion imaging is mostly utilized in the central nervous systems. Diffusion imaging in brain benefits from the sufficiently large transversal relaxation of the tissue. The diffusion in the different regions within the brain is different, which is an advantage when characterizing the brain tissue. A typical clinical application of diffusion weighted imaging is the detection acute strokes.

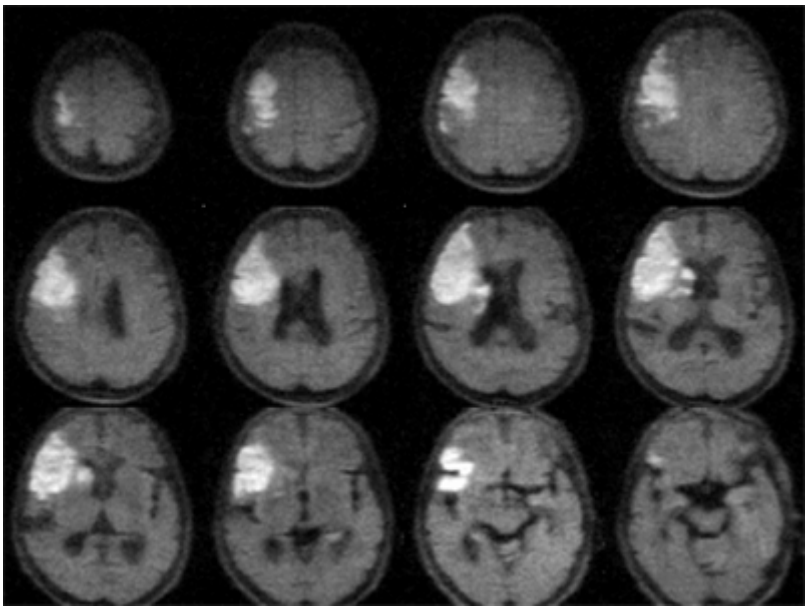

Figure 1.1: Diffusion weighted image of a stroke patient **[1]**

The destroyed regions can be detected due to the distortion of diffusion. These changes can be recognized already after a few minutes after a stroke and give information which tissue might be saved through clinical intervention.

The Brownian motion itself depends on the temperature of the underling tissue. The warmer the subject, the more mobile the protons. This rise of mobility of the protons can be detected by using diffusion imaging. The acquired data of aqueous solutions can be used for temperature assessment. E.g. using diffusion imaging in brain not only provides information of the structures of the brain, it also provides an internal reference of the temperature.

A further clinical application of magnet resonance imaging is post mortem imaging. For many ethnic, cultural or religious groups a common autopsy is not possible because of the lack of consent. The noninvasive method of post mortem imaging doesn't harm the body and will provide comparable information as a conventional autopsy. Another advantage over the common type of analysis is to avoid the contact to cadaver or tissue with harmful diseases. Post mortem imaging may also provide additional information for the autopsy. If there are any abnormalities in organs, post mortem imaging can guide the pathologist to this tissue to take some histological information, which may not be found at first morphologic sight. Furthermore the changes and distortions are avoided by removing the brain out of the cadaver, which will be a typical consequence. Imaging cadavers will also provide data, which are more comparable with the body as imaging organs after extraction [2]. Additional advantages of imaging cadaver are the repeatability and variability of the experiments. Once a conventional autopsy is done, you are not able to repeat or undo any step. Every surgical intervention will destroy the body and perhaps important information. The acquired data can

be used as often as needed without loss of details or additional information. The data could be shared with other experts who are not able to be present during an autopsy.

1.2 Objectives

This diploma thesis focused on a MRI model that explains the mobility of water protons in the human brain after death. After dying, several mechanisms are initiated that trigger cellular destruction and loss of the tissue matrix, often considered as autolysis of the brain. The progress of autolysis does not only depend on biochemical factors (enzymes, bacteria, etc.), but also on the temperature and on the post mortem delay. Additional to the information of the tissue, the temperature can be estimated using the movement of the water protons within the cerebrospinal fluid of the measured cadavers. Tofts et. al. showed a clinical application of temperature assessment of corpses which will be implemented for an internal reference. Duffusion changes in the brain related to the autolysis will be compared to diffusion properties of normal brain to develop a model which describes the dependency of temperature and postmortem delay.

2 Theory

2.1 Physical basics

Nuclear Magnetic Resonance Imaging is a procedure, which uses the material which appears most in the body: The water, more precisely the behavior of the nucleus of hydrogen in a magnetic field, is used to get information about the body. The classic model of the magnetic gyroscope in a constant magnetic field is the basic of all further research methods. In order to use this model we have to introduce the magnetic dipole moment $\vec{m}$ and the torsional moment $\vec{T}$.

$$\vec{m} = I \cdot F \cdot \vec{e_n} \qquad \vec{T} = \vec{m} \times \vec{B}$$

If we define the angular moment and the equation of motion we are able to derive the equation of motion for the magnetic gyroscope.

$$\vec{L} = I \cdot \vec{\omega} \qquad \vec{T} = \frac{d\vec{L}}{dt} \qquad \vec{m} \times \vec{B} = \frac{d\vec{L}}{dt}$$

The external magnetic field of the tomograph causes these protons to precess. The direction of L can't be said exactly. The angular velocity can be calculated using our introduced equations.

$$\omega_0 = -\frac{T}{L \cdot \sin\alpha} = -\frac{m \cdot B \cdot \sin\alpha}{L \cdot \sin\alpha} = -\frac{m \cdot B}{L}$$

The expression $\frac{m}{L}$ is called gyromagnetic ratio γ. The precession occurs in negative mathematical direction of counting, i.e. the precession is below zero. This leads to the typical convention.

$$\omega_0 = \gamma \cdot B \quad f_0 = \frac{\gamma}{2\pi}\mathrm{B}$$

After exposure to a short impulse of an electromagnetic field with the frequency of the precessing protons, the protons themselves become to a sender to and give information of their surrounding area.

2.1.1 Diffusion and self Diffusion

2.1.2 Diffusion

The material transfer from one part of a system with a higher concentration of any solution to another system with a lower concentration of the solution due to the random motion of the molecules is called diffusion. Fick described the flux of matter in his famous law. The second law of Fick describes the time and spatial dependency of the first law.

$$J = -D\frac{\partial c}{\partial x} \qquad \frac{\partial C}{\partial t} = D\frac{\partial^2 C}{\partial x^2}$$

2.1.3 Self- Diffusion

Self diffusion is the motion of molecules in no preferred direction, in contrast to the concentration gradient induced diffusion. Robert Brown rediscovered this phenomenon in 1827. Brown was a botanist and observed the movement of polls on a water drop. He noticed an uncontrolled twitch of the pollen and assumed that the motion is a sign of vitality. After realizing the effect also occurs with dust particles he stopped his researches for a sign of vitality.

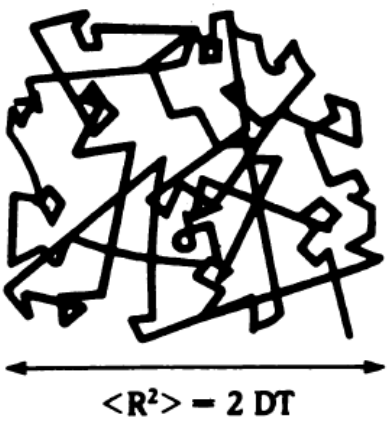

Figure 2.1: Random walk

The picture [3] *describes the random walk model of the Brownian motion. The diffusion coefficient D is responsible for the mobility of the molecule. The diffusion coefficient of pure water is 2.5 *10^-3 mm²/s at a temperature of 40°C. This is equal to a movement of 22µm in 100 ms.*

2.2 The Bloch Equation

The Bloch equations were invented in 1946 by Felix Bloch. They describe the general equation of motion for a magnetic gyroscope.

In the Cartesian coordinate system:

$$\frac{d\boldsymbol{L}}{dt} = \boldsymbol{M} \times \boldsymbol{B} \qquad \boldsymbol{L} = \frac{\mu}{\gamma} \qquad \boldsymbol{M}(t) = \sum \mu_{\boldsymbol{i}}(t)$$

$$\frac{d\boldsymbol{M}}{dt} = \gamma(\boldsymbol{M} \times \boldsymbol{B})$$

To simplify the consideration, the equations were transformed into a rotating coordinate system. Assuming that the coordinate systems rotate with the speed of ω following change will happen. The following four pictures of the coordinate system and the free induction decay were taken from the Bioimaging script of Prof. Stollberger. [4]

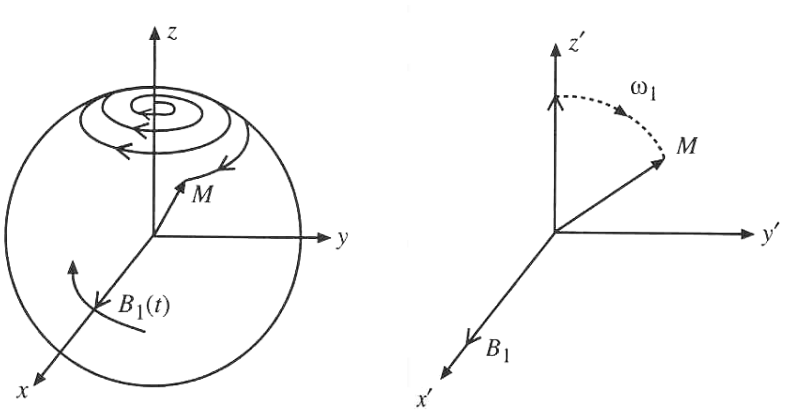

Figure 2.2: Cartesian and rotating coordinate system

The left image shows the Cartesian coordinate system. After excitation the proton is going to precess back into the magnetic field B0. If you consider that the coordinate systems rotates with the precession frequency of the proton (right image), the magnetization vector will just be flipped into the xy-area and will go back the same way. The change of the coordinate system will also affect the free induction decay FID.

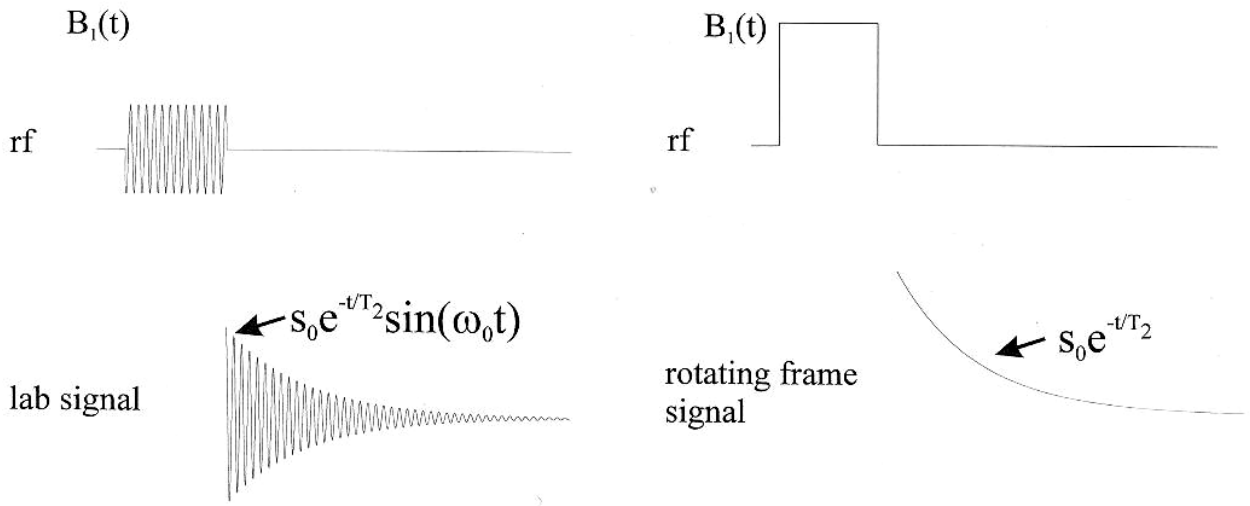

Figure 2.3: FID in different coordinate systems

As you can see, the rf impulse will be transformed into a single pulse in the rotating coordinate system. The FID also will transform into the envelope curve of the signal.

By changing the coordinate system a negative effect occurs. If the velocity of the rotating coordinates system is not exactly the same as the precession frequency. The effective magnetic field will be different to the magnetic field in the Cartesian coordinate system. This effect is called B0-Inhomogeneties.

According to the changed coordinate system and implementing the relaxation terms, the Bloch equation can be written in the rotating coordinate system.

$$\frac{d\boldsymbol{M}_{x'y'z'}}{dt} = \begin{pmatrix} -\frac{1}{T_2} & \Delta\omega & 0 \\ -\Delta\omega & -\frac{1}{T_2} & \omega_1 \\ 0 & -\omega_1 & -\frac{1}{T_1} \end{pmatrix} \boldsymbol{M}' + \begin{pmatrix} 0 \\ 0 \\ \frac{M_0}{T_1} \end{pmatrix}$$

$$\Delta\omega = \gamma B_0 - \omega \qquad\qquad \omega_1 = \gamma B_1$$

The parameters of the equation will be discussed in extended version of the Bloch equation.

The advantages of the Bloch equations are that the equations can be easily adjusted. Every term of variation is simply added to the equation. This makes it possible to calculate the diffusion by adding a diffusion term. Torrey varied the equation by adding a term, which was responsible for the displacement of the magnetization by self diffusion. The so called Bloch-Torrey Equation was formed in 1956.

$$\frac{\partial \boldsymbol{M}}{\partial t} = \gamma \boldsymbol{M} \times \boldsymbol{B} - \begin{pmatrix} \frac{1}{T_2} & 0 & 0 \\ 0 & \frac{1}{T_2} & 0 \\ 0 & 0 & \frac{1}{T_1} \end{pmatrix} \boldsymbol{M} + \boldsymbol{M_0} \begin{pmatrix} 0 \\ 0 \\ \frac{1}{T_1} \end{pmatrix} + \nabla(D \nabla \boldsymbol{M})$$

M describes the magnetization vector in a rotating coordinate system in presence of a field vector **B**. T1 and T2 are called relaxation times. T1 is describing the longitudinal relaxation (spin-lattice relaxation) and T2 describes the transversal relaxation (spin-spin relaxation). The diffusion coefficient is represented by D.

2.3 Quantitative analysis of diffusion weighted imaging.

To measure the diffusion coefficient at least two measurements have to be done. One measurement with diffusion weighting and one measurement without diffusion weighting are needed. [5] The anisotropy of the tissue is responsible for the value of the diffusion coefficient, i.e. depends on the diffusion weighting (values of the strength of the diffusion gradient, the Stejskal – Tanner parameter and the diffusion directions). Therefore it is more appropriate to introduce the apparent diffusion coefficient which only depends on the diffusion time and the b-factor. The b-factor is the relation between the self diffusion coefficient and the magnetic resonance signal. When the parameters $S(TE, 0)$, $S(TE, b)$ and the b-factor are known for all voxel, a diffusion map can be produced where each voxel represents the value of the average diffusion coefficient.

2.3.1 Diffusion Tensor

The diffusion tensor is described by nine elemements

$$\boldsymbol{D} = \begin{pmatrix} D_{xx} & D_{xy} & D_{xz} \\ D_{yx} & D_{yy} & D_{yz} \\ D_{zx} & D_{zy} & D_{zz} \end{pmatrix}$$

D_{xx} , D_{yy} and D_{zz} define the diffusion constants on the main axes, whereas the diagonal terms represent the diffusive flow, which is affected by the concentration gradient

$$\boldsymbol{D}\varepsilon_i = \lambda_i \varepsilon_i = \lambda_i \boldsymbol{I} \varepsilon_i, \qquad i = \{1,2,3\}$$

$$\begin{pmatrix} D_{xx} & D_{xy} & D_{xz} \\ D_{yx} & D_{yy} & D_{yz} \\ D_{zx} & D_{zy} & D_{zz} \end{pmatrix} \begin{pmatrix} \mathcal{E}_{ix} \\ \mathcal{E}_{iy} \\ \mathcal{E}_{iz} \end{pmatrix} = \lambda_i \begin{pmatrix} \mathcal{E}_{ix} \\ \mathcal{E}_{iy} \\ \mathcal{E}_{iz} \end{pmatrix}$$

$\mathcal{E}_{ix}$, $\mathcal{E}_{iy}$ and$\mathcal{E}_{iz}$ are the eigenvectors of the diffusion vectors, which represent the directions of the uncorrelated molecular displacement. λ_1, λ_2 and λ_3 are the corresponding apparent diffusion coefficients, i.e eigenvalues of the diffusion tensor. The combinations of the eigenvalues and eigenvectors are unique and represent the diffusion properties of the samples.

2.3.2 Mean Diffusivity

The easiest way to combine the parameters is the mean diffusivity.

$$MD = \frac{\lambda_1 + \lambda_2 + \lambda_3}{3}$$

The maps of MD do not show a great contrast but the diffusivity is noticeable very well.

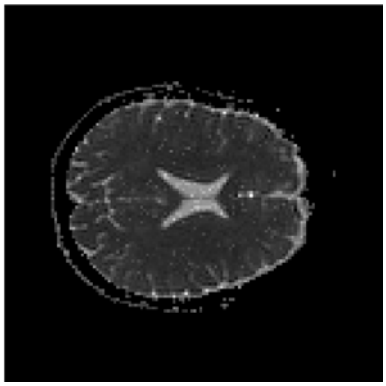

Figure 2.4: MD map of the brain calculated in Matlab

2.3.3 Fractional Anisotropy

The big advantage of the fractional anisotropy map is the high contrast of the tissue. It is very easy to interpret with a high visual impact.

$$FA = \frac{\sqrt{(\lambda_1 - \langle \boldsymbol{D} \rangle)^2 + (\lambda_2 - \langle \boldsymbol{D} \rangle)^2 + (\lambda_3 - \langle \boldsymbol{D} \rangle)^2}}{\sqrt{\lambda_1^2 + \lambda_2^2 + \lambda_3^2}}$$

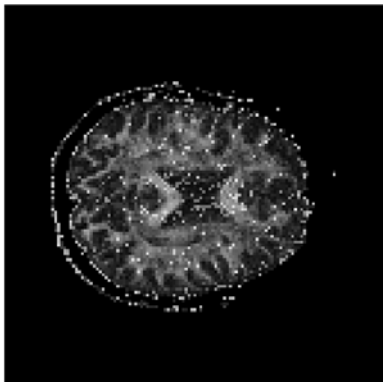

Figure 2.5: factional anisotropy map calculated from the same data set

2.3.4 Volume ratio

Volume ratio is low, if the anisotropy is high, i.e. the white matter will appear darker than the gray matter of the brain.

$$VR = \frac{\lambda_1 \lambda_2 \lambda_3}{MD}$$

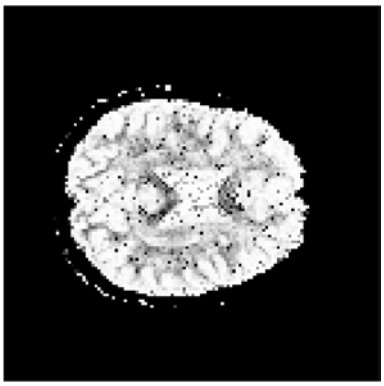

Figure 2.6: Calculated volume ratio of the same region.

2.4 Temperature assessment using MR

The thermal therapy of benign and malignant diseases using a minimally invasive therapy benefits from magnet resonance image guidance [6] The MRI provides maps with good temporal and spatial properties without invasiveness. One goal of the guided thermal therapy is to control the treatment outcome by using real time temperature mapping.

T1 and T2 relaxation, the proton density, the magnetization transfer, the diffusion coefficient and the proton resonance frequency were used for temperature measurement. All those parameters show sensitivity to the temperature. The way of assessing the temperature can be absolute and relative. Relative assessment uses a reference data which is compared to the acquired data which was measured under known conditions.

2.4.1 Proton Density

The proton density directly depends on the magnetization M0. The relation between the magnetization and the proton density is determined by the Boltzmann distribution.

$$PD \propto M_0 = \frac{N\gamma^2 h^2 I(I+1)B_0}{3\mu_0 kT} = \chi_0 B_0$$

N is the number of spins,γ is the gyromagnetic ratio, h is the Plank's constant, I is the quantum number of the spins, μ_0 is the permeability of the free space, k is the Boltzmann constant, T is the absolute temperature of the sample B_0 is the magnetic field and χ_0 is the susceptibility.

The relation of the susceptibility and the temperature is known as Curie Law.

$$\chi_0 \propto \frac{1}{T}$$

By knowing the magnetization of the sample it is possible to assess the temperature changes through the Boltzmann thermal equation. It is important to know that the proton density of the sample does not change with the measurement, but the susceptibilities will reflect the ratio of the parallel and antiparallel spin populations which relates to the temperature. The sensitivity of the proton density dependent temperature assessment is between 37°C and 80°C. The signal-to-noise ratio has to be very high to assess reliable values below the sensitivity range. Also long repetition times are needed to eliminate the effects from the T1 relaxation times.

2.4.2 T1 Relaxation times

The temperature dependence of the dipole interactions of macromolecules and water molecules relies on the translational and rotation motion. This relation affects the T1 relaxation time.

$$T_1 \propto e^{\frac{E_a(T_1)}{kT}}$$

E_a is the activation energy of the relaxation process. The T1 relaxation time depends linearly to the temperature in a small temperature range. The longitudinal relaxation time, depending on the temperature can be described as.

$$T_1(T) = T_1\left(T_{ref}\right) + m \cdot (T - T_{ref})$$

m is an empirically determined value for tissue. The accuracy of measuring and extracting T1 is responsible for the quality of the T1 based assessment of temperature. The quantification of the temperature is rather difficult. The temperature coefficient of the T1 acquired data is normally not known and individual for each tissue.

2.4.3 T2 Relaxation time of water Proton

The increase of the T2 relaxation time with increasing temperature has also been observed in aqueous solutions and is similar to the temperature dependency of T1 relaxation. The T2 relaxation time in tissue is significantly reduced and the dependency on temperature is masked by other factors.

2.4.4 Temperature assessment using diffusion

As mentioned before, the diffusion coefficient depends on the temperature and the method relies on this relation. The relation of the diffusion coefficient and the temperate can be shown in the equation.

$$D \approx e^{\frac{E_a(D)}{kT}}$$

The dependency of temperature is described by

$$\frac{dD}{DdT} = \frac{E_a(D)}{kT^2}$$

Therefore following temperature change can be derived.

$$\Delta T = T - T_{ref} = \frac{kT_{ref}^2}{E_{a(D)}}\left(\frac{D - D_{ref}}{D_{ref}}\right)$$

The sensitivity of the diffusion based temperature assessment is very high. The problem of this method is the high motion sensitivity, which is a major problem in vivo. Therefore very fast acquisition methods, such as single shot sequences are needed. Another problem is the nonlinearity of the temperature dependency of diffusion in tissue, when the conditions change (heat induced changes, scar tissue, ischemia).

2.4.5 Temperature measurement using magnetization transfer

To saturate the protons in macromolecules and water, which is bound to macromolecules, a spectrally selective RF pulse is used. Usually these protons are not visible, but they transfer their magnetization to the water molecules during this RF impulse. The measured signal will be reduced due to this transferred magnetization. The transfer process is temperature dependent and can be used for temperature assessment.

Protons resonance shift of water protons

The protons resonance shift was first implemented for spectroscopy, before this effect was used for temperature measurement. The nucleus field is determined as

$$B_{loc} = B_0 - B_{0s} = (1 - \sigma)B_0$$

σ is called screening or shielding constant and depends on the chemical environment.

$$\omega = \gamma B_0(1 - \sigma)$$

The hydrogen bounds are responsible for a distortion the electronic configuration. This distortion leads to a reduced electronic screening of the neighbored molecules. The temperature will stretch those hydrogen bounds or even break them. Therefore more screening of the H- nucleus are possible, which leads to a higher attenuation of the local magnetic field and a lower resonance frequency. The temperature range for this assessment method ranges from -15°C to 100°C.

In addition there are temperature sensitive contrast agent based methods to acquire the temperature, which will be not discussed in this thesis.

2.5 Diffusion Weighted Imaging

The needed profiles for the reconstruction of the image are acquired with one single shot. Therefore one excitation is used to generate as many echoes as possible by switching the gradient system. The single-shot spin echo-planar imaging sequence provides a method to measure the self-diffusion of protons with minimizing the effects of the spin-lattice relaxations. The sequence needs a high homogeneity and very long T2 relaxation time to ensure a sufficient data acquisition.

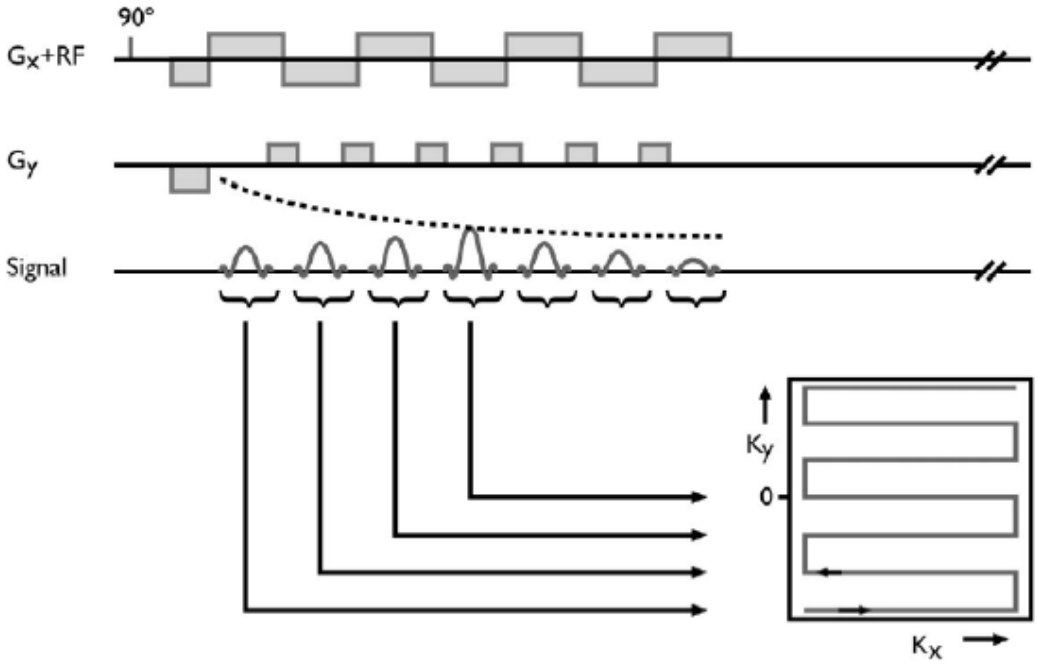

Figure 2.7: Diffusion Sequence

The figure was taken from the Bioimaging script [4] and describes the way how the echoes are generated and how the k–space is filled. After a single 90° RF pulse several gradient switches are used to refocus the spins in order to get an echo signal. Currently this sequence is the fastest method for magnet resonance imaging. The speed enhancement of the EPI sequence is direct proportional to the total amount of acquired echoes. The number of the reading gradient impulses is called EPI-factor. In case of single shot-EPI, this factor equals to the size of the matrix in the direction of the phase coding gradient. The gradient Gy is used to switch to the next line of the k-space. Filling the whole matrix this way (with only one excitation) leads to several artifacts. Phase errors induced through field inhomogeneities or chemical shift accumulate from k-line to k-line.

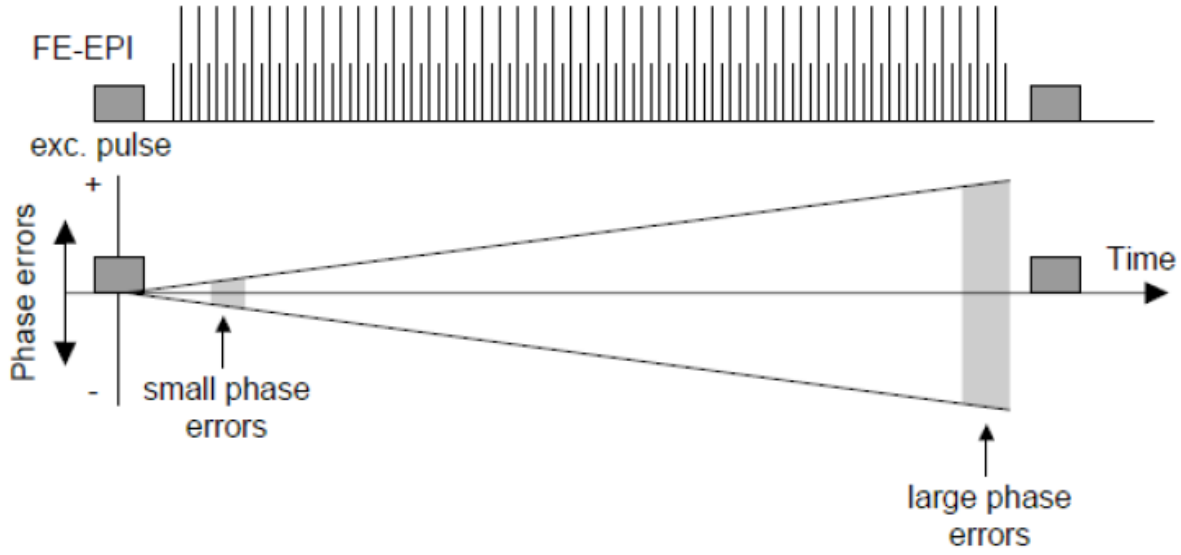

Figure 2.8: appearance of phase errors

The image, also taken from the Bioimaging script, shows the propagation of the phase error. The small phase error in the beginning of the excitation will rise during the measurement. To avoid this phase error, the data should be acquired as fast as possible.

The scan time of echo planar imaging can be calculated with the following formula:

$$T_{scan} = ES \cdot N_{phasencode} \cdot N_{Averages}$$

The maximal scan time should be below 100 ms. Another problem of echoplanar imaging happens, if the T2-relaxation time is much shorter than scan time. In that case, the magnet resonance signal will disappear before the k-space is filled. Especially the outer data points of the ky values will be missing. This leads to blurring effects on the image. A further artifact occurs, if there are any lacks of the gradient system or if there is a field inhomogeneity. These effects may lead to errors in the time control of the even and odd echoes. The Fourier transform will translate them into phase errors and this will lead to ghosting.

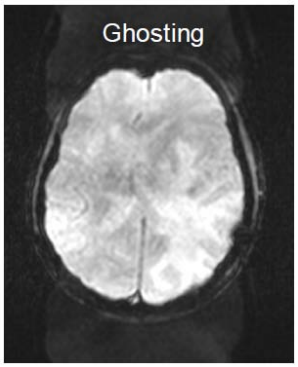

Figure 2.9: Nyquist-ghosting effect.

Another reason for ghosting artifacts in other body parts may be time dependent B0 inhomogeneities. This could be induced by breathing or through heart beats.

3 Methods

3.1 Used System

The data sets were acquired with a Siemens Magnetom Trio. This is a clinical magnet resonance tomograph with a static field of 3 T. The maximal effective amplitude of the gradient system in all directions is 72 mT/m. The maximal slew rate of the Siemens Magnetom is 346 T/m/s.

3.2 Thermometry – first model

The paper of Paul Tofts describes one possible method to assess the temperature using a Flair sequence. He used a GE Medical systems (Milwaukee, WI) 1.5 T imager with a birdcage transmit-receiver head coil to measure the diffusion coefficient. The link between diffusivity and temperature was the research of R. Mills [7]. He used the magnetically stirred diaphragm cell method to determine the diffusion constant of water. This technique was originally developed by Stokes. This paper also describes the dependence of self diffusion on different temperatures. Tofts derived an equation out of the results from Mills to convert the diffusion coefficient directly into a temperature value.

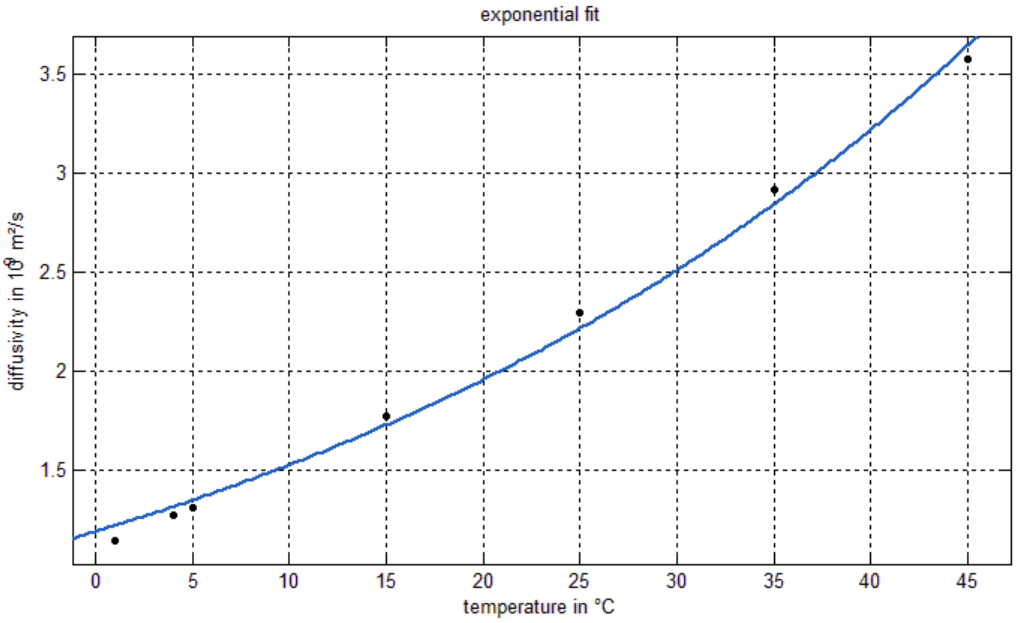

Figure 3.1: Exponential fit of the diffusivity dependency on temperature

This image shows the behavior of diffusivity due to temperature. Literature shows the exponential rise of the diffusivity related to temperature, which will be discussed later. Therefore we used an exponential fit to interpolate the curve between the data points.

The acquired data sets contain images of corpses and reference images of living subjects. To compare the different data sets it is necessary to adjust these images. It has to be ensured that the compared regions are exactly the same anatomical structures and that the distortions through eddy current and head movement of references are removed. The FMRIB Software Library was used to registrate and to eddy correct the basic data.

Eddy is a useful method of FSL to correct eddy currents and moments distortions in diffusion data. The tool models the effects of those distortions and corrects the original data with this modeled data. [8]

TBSS – Tract Based Spatial Statistic is a tool, which uses the information about anatomical connectivity in the brain by measuring the anisotropic diffusion of water in white matter tracts. Initial position for this procedure is the fractional anisotropy maps of all images. TBSS tuned nonlinear registration followed by projection onto an alignment-invariant tract representation. This representation is called mean FA skeleton. [9]

After these corrections the temperature of the acquired data has to be adjusted. The cadavers have different temperatures and therefore a comparison of diffusivity is not possible. Related to the paper of Mills we calculated a correction factor which will correct our data to 37°C reference temperature.

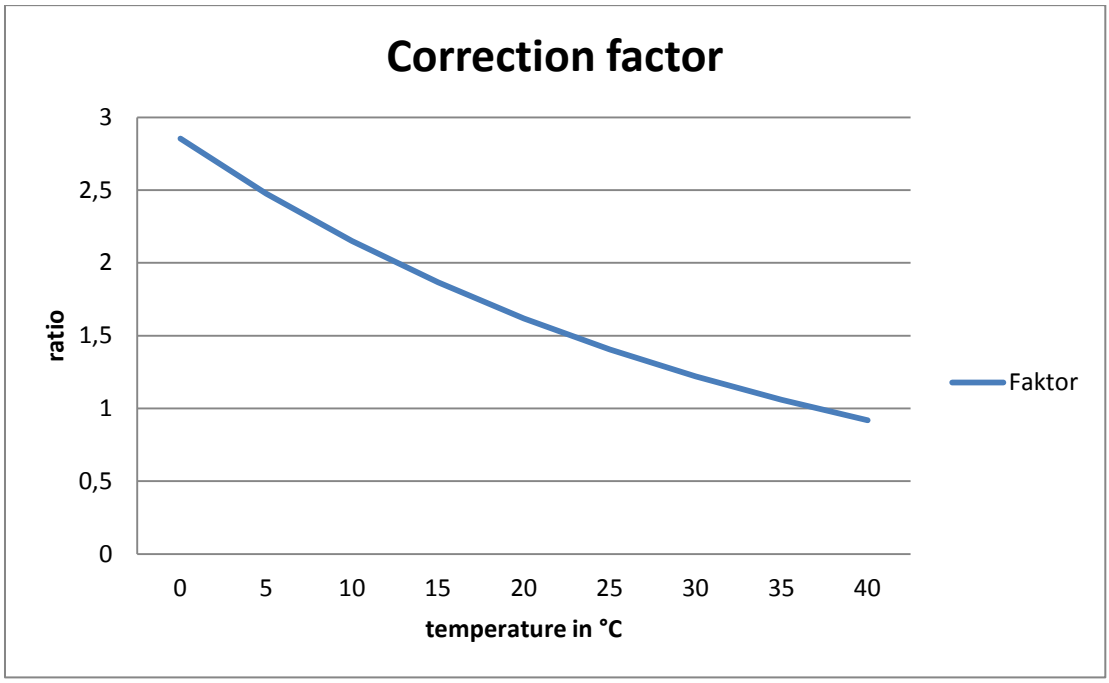

Figure 3.2: Correction factor

This plot shows the different factors for the temperature of the corpses. The higher the temperature of our sample is, the lower the factor has to be. As you can see, there is no correction at 37°C

3.3 Thermometry, extended model

The first model of thermometry postulates that the cerebrospinal fluid behaves like water. This assumption is correct for healthy people. If there are any inflammations or autolysis effects after death, the model has to be adjusted.

Daniel Wyler, Walter Marty and Walter Bär [10] show the correlation between the post-mortem cell content of cerebrospinal fluid and time of death. They performed a lumbar puncture on patients who died in the hospital. Only corpses without any lesions of the central nervous system are used for this study. To show the effect of temperature, they divided the corpses into two groups. One group remains at 20°C room temperature and a second group was placed in a cold-storage chamber at 4°C immediately after death. Both groups are handled in an analogous way, to provide comparable results. All samples, which were contaminated with blood (artificial bleeding during lumbar puncturing), had been disqualified for the determination of cell content.

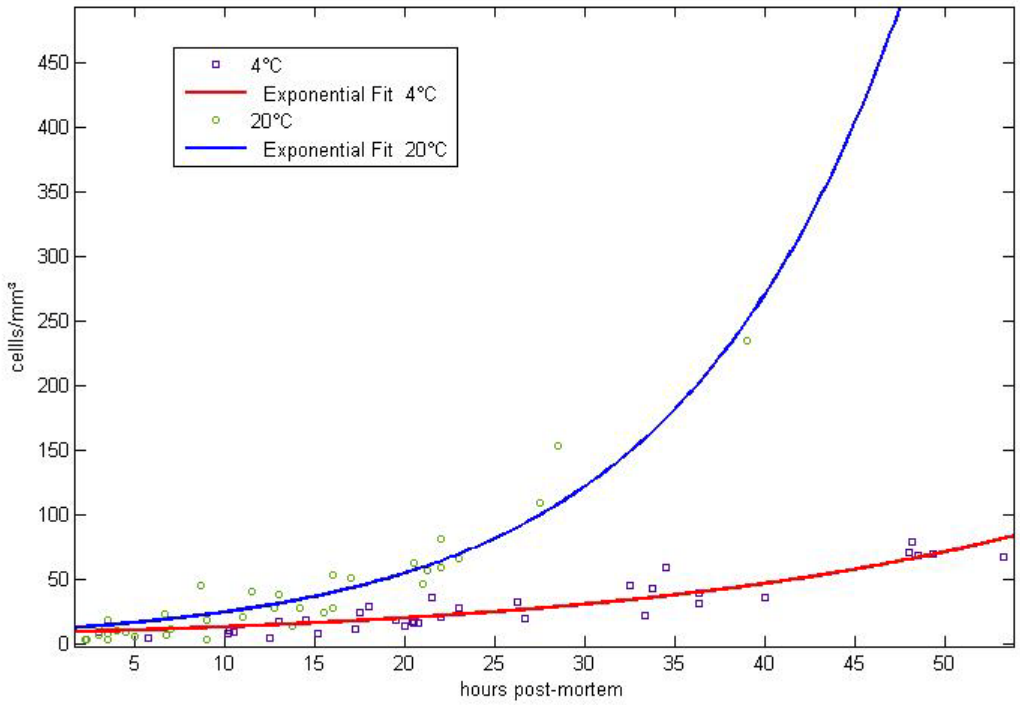

Figure 3.3: Cell density dependency on post mortem delay

The figure shows the relation between cell density and post-mortem hours. The diagram clearly shows that the temperature takes a major role how many cells are transported into the cerebrospinal fluid. The data points are fitted exponentially to provide a defined cell density for each time after death.

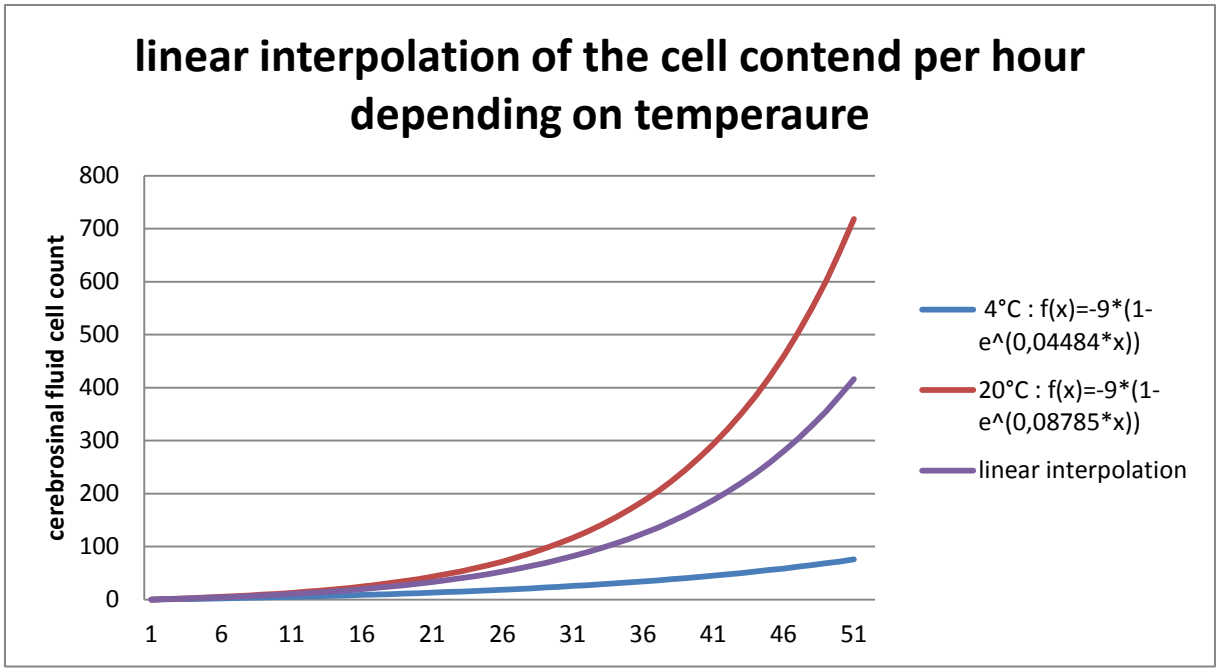

Figure 3.4: linear interpolation of the cell contend per hour depending on temperaure

Depending on the results of the study from Wyler et al. it was possible to interpolate a function for different temperate dependency. This function can be used for assessments of the cell density. Therefore the exponent is linear interpolated to provide data for any temperature.

Takanori Sasaki et al [11]. describes the dependency of the apparent diffusion coefficient of Ramos Cells on cell density using Bio-phantoms. He used Ramos cells which were encapsulated into bio-phantoms. These bio-phantoms were placed into a phantom container filled with PBS (phosphate-buffered saline). The phantom container remains in a water bath which was heated to a temperature of 37°C. After first run of imaging the Ramos cell's membrane was destroyed by sonication and the measurement was repeated.

Figure 3.5: Experimental arrangement of Takanori

The figure shows the phantoms and the methods of his study and was taken from their released paper. (A) Frontal view of the bio- phantom. (B) Lateral view of the bio-phantom. (C) The phantom container containing the bio-phantoms. (D) MR imaging using a head coil in a Achieva, Philips Electronics Japan 1,5 T magnet resonance tomography

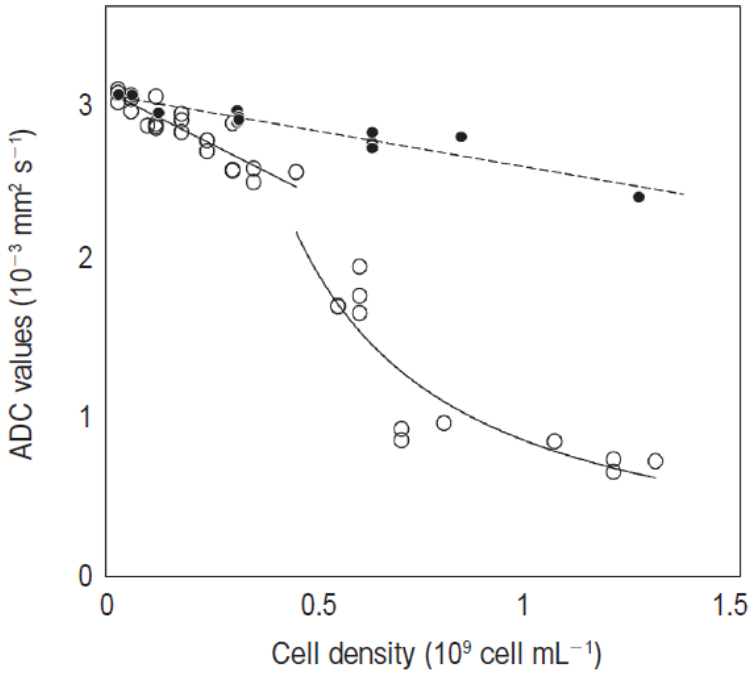

Figure 3.6: Dependency of the apparent diffusion constant on cell density

The figure shows the relationship between the cell density and the apparent diffusion coefficient. The black painted curls show the sonicated cells. There is a significant change on the ADC values after destroying the membrane. The ADC values also decreased as cell density decreased.

The results of Takanori Sasakis' leads to the assumption that the ADC value decreases linearly according to the cell density and there also has to be a linear correlation between the size of the cells and the decreased diffusivity. Combining this with the knowledge of cell content we are now able to create a model, which can be used for thermometry.

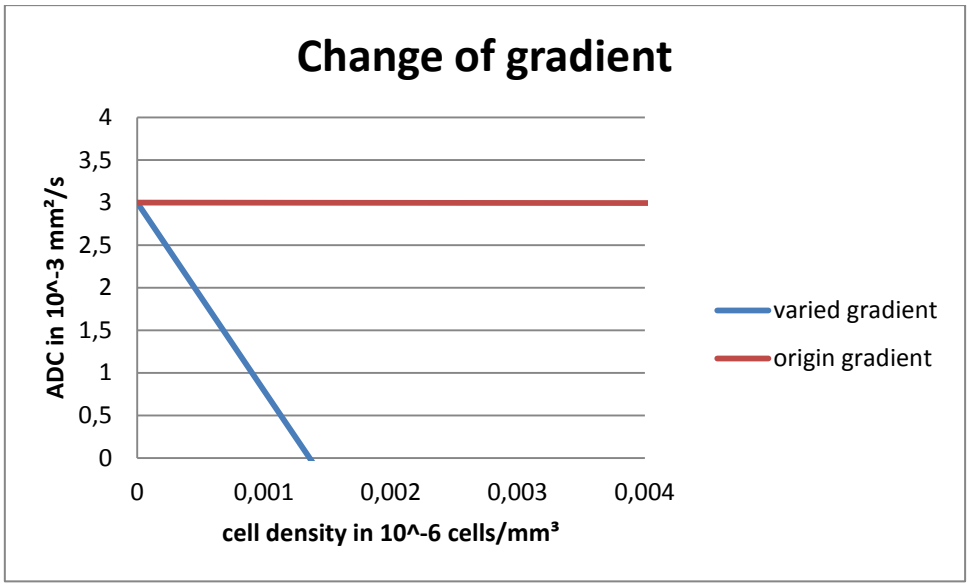

Figure 3.7: Gradient change of the ADC dependency on cell density

The figure shows how the gradient of the relation between cell density and apparent diffusion efficient has to be adjusted to assess the temperature of a corpse. The gradient was found empirically out of the acquired temperature corrected data sets. All data sets were corrected to 37 °C.

4 Results

4.1 Manually taken data

Basis of all calculation and the results were the data taken from the Ludwig Boltzmann Institute of clinical-forensic imaging. Those data consists the basic information of the corpses.

- Temperature of the body before scan (rectal measured)
- Temperature of the body after scan (rectal)
- Post mortem delay
- Trauma

Additional to this manually taken data, two phantoms were added into the scanner. The two phantoms, small tubes, were filled with water and should have helped to calculate the temperature. One of the phantoms had a temperature of 20 °C and the other 8 °C.

Studiennr.	Geb.datum	Datum Bildgebung	Trauma	Scanabbruch	t Tod-MRT	Bemerkungen	T präScan	T postScan	TPh1prä	TPh2prä	TPh1post	TPh2post
200-09	20.09.1970	29.04.2009				Test, Scan 2&3: 29.05./01.06.09;						
201-09	06.08.1947	26.05.2009				Test,						
202-09	09.09.1950	29.05.2009			50 +/- 2		6.2					
203-09	20.09.1970	29.05.2009				Organscan	Raum					
204-09	20.09.1970	01.06.2009				Organscan 2	6.5	12	7.4	20.5	17.3	18.4
205-09	24.02.1928	03.06.2009			~ 61		5.5		7.6	22.6	19.3	20.5
206-09	04.01.1961	03.06.2009			64 +/- 2		4.6	-	8.7	20.5	21.4	21.7
207-09	06.08.1947	15.06.2009				Organscan	7	17.4	8.8	25.3	20.6	21.8
208-09	09.09.1950	22.06.2009				Organscan	8.2	15.8	7	23.9	19.5	20.5
209-09	24.02.1928	06.07.2009				Organscan	8.8	15.8	7.2	24.6	20.2	20.6
210-09	26.04.1919	08.07.2009	x	o			7.1	-	7.3	22.7	20.9	21.3
211-09	04.01.1961	13.07.2009				Organscan	9.4	16.6	7.5	22.7	20.3	20.5
212-09	24.08.1943	10.08.2009		o			8.7	-	9.5	26.5	18.8	19.4
213-09	15.06.1947	29.10.2009			30 +/- 2		12.2	13.3	10.3	21.7	20.2	21.3
214-09	12.06.1949	06.11.2009			26		18.2	19.1	7.4	22.3	20.1	20.5
215-09	15.06.1947	24.11.2009				Organscan	6.3	17.4	6	22.6	18.9	19.7
216-09	12.06.1949	30.11.2009				Organscan	9.2	18.1	15.8	22.7	20.1	20.4
217-09	28.06.1945	18.12.2009			36		15.5	15	6.9	21.1	21.3	21.8
219-10	19.03.1953	04.01.2010			~ 12		23.7	24.7	7.3	24	23.1	23.7
220-10	23.05.1940	12.01.2010			40		11	12.1	6.9	23.2	20.8	21.2
221-10	21.03.1931	15.01.2010	x		53		6.3	10.1	8	23.4	19	19.4
222-10	28.06.1945	22.01.2010				Organscan	4.5	14.7	6.3	23.5	17.7	17.8
223-10	19.03.1953	29.01.2010				Organscan	4.2	15.1	7.3	23.1	17.6	17.7
224-10	28.07.1943	03.02.2010		o	29-53		15.7	15	6.6	23.7	20.6	21.5
225-10	23.05.1940	05.02.2010	x			Organscan	3.6	14	7.2	24.5	17.3	17.7
226-10	22.06.1965	16.02.2010		x	-		-	-	-	-	-	-
227-10	21.03.1931	19.02.2010				Organscan	4.4	16.5	6.4	23.7	19	19.6
228-10	02.09.1956	09.04.2010	x		18-19		21.6	21.3	7.2	22.5	23.1	23.2
229-10	02.09.1956	15.05.2010	x			Organscan	6.7	20.3	-	-	-	-
232-10	20.08.1929	31.03.2010			28		15.2	16.3	5.2	21.9	22.4	23.1
233-10	28.02.1935	01.06.2010			29		17.9	16.9	9.8	22.3	23.5	23.5
234-10	17.04.1954	08.06.2010	x		50		11.2	13	7.1	23.1	21.9	22.7
133-10	20.06.1972	16.06.2010	x		24		21.7	20.4	12.6	24.2	23.5	23.6
236-10	20.08.1929	25.06.2010				Organscan	6.7	15.9	-	-	-	-
237-10	28.02.1935	02.07.2010	x			Organscan	7.6	17.6	-	-	-	-
238-10	20.06.1972	15.07.2010	x			Organscan	8.3	19	-	-	-	-
239-10												

Table 4.1: Manually taken data

All manually taken data were collected in above shown datasheet. The whole measurement of the corpses consists of many different sequences. The diffusion sequence was one of the last sequences which was taken with the scanner. Therefore a change in the temperature

was expected. The room temperature within the scanner realm was 20 °C and the volume of the two phantoms was very small, so that a steady state of the temperature was reached quite fast. The last two columns show, that both phantoms reached this temperature in the end of the measurement. A further aspect of the temperature was that the skull isolates the brain very well. The temperature was measured rectally and might be different to the brain in the end of the scan. Another problem of the manually measured data was the inaccuracy of the clinical thermometer. Some of the measured corpses had a lower body temperature at the end of the scan, which was not possible because of the higher room temperature.

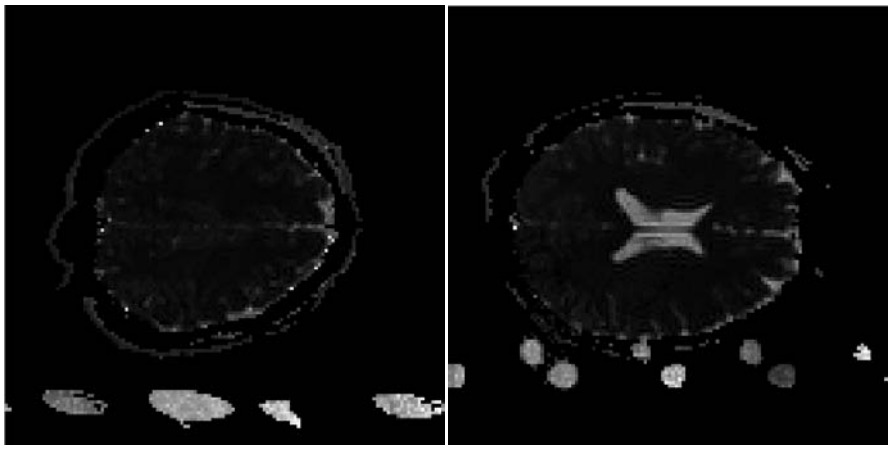

Figure 4.1: Calculated diffusion maps using Matlab

These figures show the mean diffusivity maps of two different corpses' brain. The bright locations in the bottom of the images are the phantoms. The scanner automatically corrects the phasing error of the brain, but not the phasing error of the phantoms. This leads to ghosting effects in some of the data sets. The corpses were scanned in the body bag. This is reason why an exact placement of the phantoms was not possible. In the left image the tubes are more angular, which leads to a bigger diameter in the slices.

4.2 Temperature assessment

According to Tofts study about the diffusion dependency, the findings of J. H. Simpson et al. [12] were used to fit a function for calculating the temperature. Simpson measured the self diffusion of oxygen-free water from the range 0° - 100°C

T (°C)	$D\times10^5$ (cm²/sec)	T_1 (sec)	$\frac{D\eta}{T}\Big/\left(\frac{D\eta}{T}\right)_{25°C}$	$\frac{T_1}{D}\Big/\left(\frac{T_1}{D}\right)_{25°C}$	$\frac{T_{1\eta}}{T}\Big/\left(\frac{T_{1\eta}}{T}\right)_{25°C}$
0	0.97	1.59	1.00	1.04	1.03
5	1.16	1.88	0.99	1.02	1.02
10	1.36	2.20	0.98	1.02	1.01
15	1.58	2.55	0.98	1.02	1.00
20	1.85	2.95	0.99	1.01	1.00
25	2.13	3.37	1	1	1
30	2.46	3.82	1.02	0.98	1.00
35	2.79	4.30	1.02	0.97	1.00
40	3.14	4.76	1.03	0.96	0.99
45	3.52	5.27	1.04	0.95	0.98
50	3.94	5.77	1.05	0.93	0.97
55	4.37	6.78	1.06	0.91	0.96
60	4.82	6.81	1.06	0.89	0.95
65	5.30	7.36	1.07	0.88	0.94
70	5.78	7.91	1.07	0.86	0.93
75	6.27	8.49	1.07	0.86	0.92
80	6.81	9.10	1.08	0.84	0.91
85	7.26	9.70	1.07	0.84	0.90
90	7.75	10.30	1.06	0.84	0.89
95	8.20	10.95	1.05	0.84	0.88
100	8.65	11.55	1.03	0.84	0.87

Table 4.2: Measured self-diffusion coeffiecents of water

The table was taken from Simpsons' paper and shows the measured values of the different dependencies of temperature. For acquiring the data he used a nuclear magnetic resonance fee precession technique.

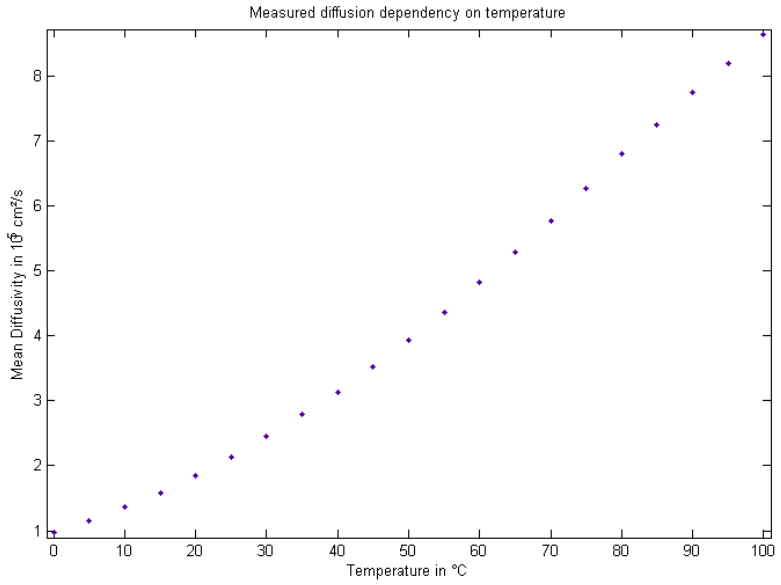

Figure 4.2: Diffusion dependency on temperature according to Simpson

The diagram was generated out of his measured table. In matlab it was possible to compare many ways of generated functions, which were representing the data points. Different types of fits showed, that a cubic fit matches the values best. The sum of squares due to error is about 0.01488 with R^2 of 0.9999.

Nr.	mean value	standard deviation	n	standard deviation in %	MD in 10^-3 mm²/s	calculated temperature in °C	measured temperature in °C
133	0,0015696	0,00019789	408	12,60766437	1,5696	10,73067387	21,7
201	0,0013718	9,33999E-05	374	6,808565389	1,3718	6,311692934	missing
202	0,0011165	5,84656E-05	438	5,236504254	1,1165	0,158599222	missing
205	0,0013009	6,69889E-05	938	5,149428088	1,3009	4,65585241	5,5
206	0,0013739	0,000144483	428	10,51624572	1,3739	6,360140785	4,6
213	0,0013129	0,000100581	251	7,660941427	1,3129	4,938885364	12,2
214	0,0013158	0,000164761	235	12,52172063	1,3158	5,007113694	18,2
217	0,0012842	0,000178347	78	13,88779006	1,2842	4,260055554	15,5
219	0,0016148	0,00015499	914	9,598080258	1,6148	11,70112922	23,7
220	0,0012878	8,31411E-05	276	6,456058394	1,2878	4,345565624	11
221	0,0013049	5,57673E-05	714	4,273683807	1,3049	4,750323801	6,3
228	0,0017691	0,000153862	730	8,697185009	1,7691	14,91119324	21,6
232	0,0015517	8,6372E-05	244	5,566282787	1,5517	10,34243469	15,2
233	0,0013755	0,000184373	197	13,40408579	1,3755	6,397030658	17,9
234	0,0014228	0,00014214	150	9,990167276	1,4228	7,478760542	11,2

reference group	mean value	standard deviation	n	standard deviation in %	MD in 10^-3 mm²/s	calculated temperature in °C
CL	0,0019281	0,000104996	305	5,44554743	1,9281	18,06358675
KR	0,0020492	9,46558E-05	971	4,619159184	2,0492	20,36770528
MC	0,0018428	0,000162237	132	8,803836553	1,8428	16,39113982
ML	0,0019378	0,000145388	246	7,5027299	1,9378	18,25111876
MS	0,0018525	0,00014883	130	8,034008097	1,8525	16,58347327
PE	0,0020574	6,89978E-05	460	3,353638573	2,0574	20,52088233
RW	0,0019004	5,13499E-05	587	2,702056935	1,9004	17,52511163
SG	0,001982	0,000122005	321	6,155645812	1,982	19,09899105
SR	0,0018847	0,000142031	173	7,536021648	1,8847	17,21795151

Table 4.3: Calculated temperatures using temperature maps of matlab

The tables show the calculated temperatures. The data sets were eddy current corrected by FSL and mean diffusivity maps are calculated. Ensuring a correct temperature assessment each region was manually selected. The selected regions contain mainly the cerebral ventricle system. In order to exclude susceptibility effects the outer regions of the ventricle were not taken. The low standard deviation shows that the selected regions were very homogeneous. In the last two columns of the above shown table the calculated temperature is compared to the measured temperature. Unfortunately not all data sets are complete. At the time of data acquisition the importance of those data was not known and a retry of the measurement was not possible due to ethical reasons. It is noticeable that the calculated temperature is lower than the measured temperature in all cases. The different deviations to the measured temperature lead to the assumption that the post mortem interval is responsible for them. In the following table the same model was used to assess the temperature of a reference group. All temperatures were much lower than expected. The mean difference to the normal body temperature is 18.77 °C. Because of the similar results of the assessed values, a systematical error was assumed.

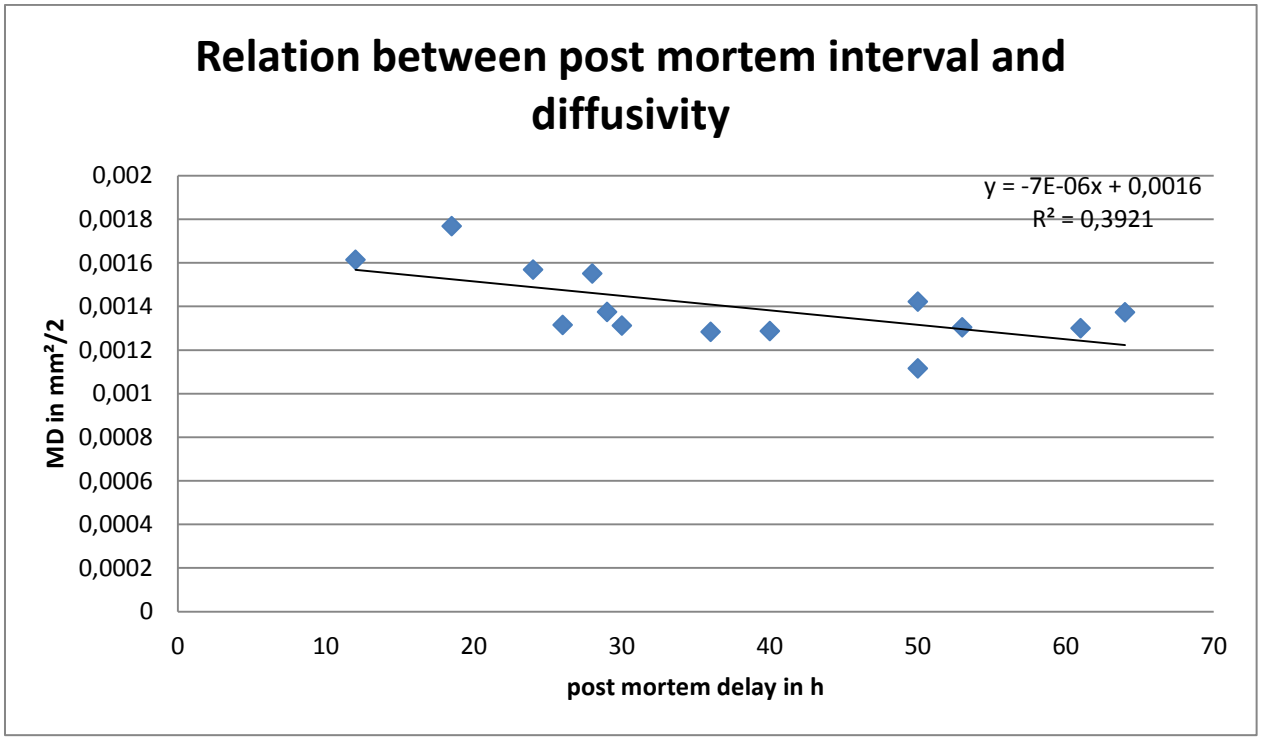

Figure 4.3: Relation between post mortem interval and diffusivity

The next step to evaluate the error of the temperature difference was to analyze the influence of the post mortem interval on the diffusivity. The same values of mean diffusivity as before were taken to see the relation to the moment of death. The attenuation of the diffusivity due to the post mortem delay is quite low. Contrary to the assumption that the

autolysis effects cause a rising of diffusivity, no evidence point to that assumption. This leads to control the independency of the two variables time of death and temperature.

No.	temperature assessed by knowing the diffusivity in °C					
	Liquor		Phantom1		Phantom2	
	mean value	std. deviatio	mean value	std. deviatio	mean value	std. deviation
133	14,7	2,149	Ghost			
201	7,473	1,595	22,027	5,153	25,529	4,59
202	6,858	1,0895	16,492	2,689	18,243	3,09
205	4,5076	0,802				
206	7,887	0,9235	Ghost			
213	6,3211	1,875	19,673	3,388	23,299	4,294
214	6,458	4,191	Ghost			
217	9	4,726	Ghost			
219	14,129	3,606	Ghost			
220	5,543	1,3227	Ghost			
221	5,1311	1,6128	Ghost			
228	17,091	2,2704	Ghost		3	
232	12,819	2,783	29,371	6,1766	26,521	4,6625
233	10,087	2,528	42,701	8,6217	50,077	10,7823
234	10,509	1,627	20,724	3,61966	20,73	2,76135

Table 4.4: Phantom measurement

The table shows the temperature assessment in the two phantoms and the liquor. The mean diffusivity maps were transformed in temperature maps and the values were directly calculated in matlab and not eddy current corrected by FSL. This is the reason why the temperatures differ from earlier tables. The regions were selected manually using MRIcro. Ghost artifacts of the phantoms leaded to exclude the sample.

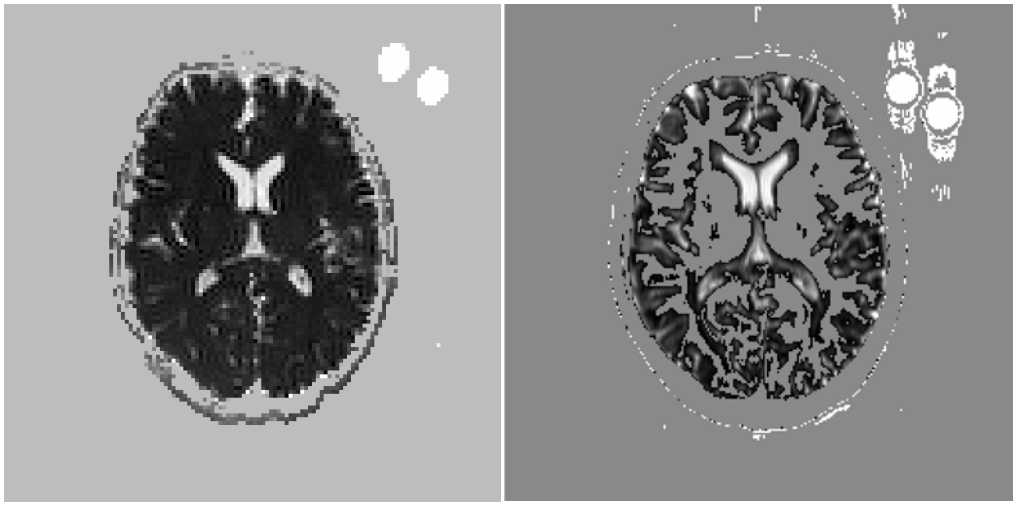

Figure 4.4: T1 and diffusion temperature maps

The images show the calculated temperature maps. The two points in the right upper corner of each image are the phantoms. The left image shows the temperature map of the diffusion image data set. The brighter the region lights up, the warmer is the region. Same behavior can be found on the right image, which is calculated out of a T1 weighted imaging sequence. Comparing the different methods to acquire the temperature both results were confronted with the manual taken measurement.

No.	temperature assed by knowing the T1 relaxation time in °C (first sequence)						temperature assed by knowing the T1 relaxation time in °C (after one hour scan time)					
	Liquor		Phantom1		Phantom2		Liquor		Phantom1		Phantom2	
	mean value	std. deviatio	mean value	std. deviatio	mean value	std. deviation	mean value	std. deviation	mean value	std. deviation	mean value	std. deviation
133	21,332	3,365	26,442	4,192	29,217	4,008	21,371	3,0736	27,594	3,903	35,094	6,094
201												
202												
205	20,322	2,789					18,262	2,073				
206	16,634	1,9833	18,112	1,687	18,975	2,3875	19,113	1,831	19,985	2,7866	19,989	2,901
213	10,124	1,074	18,309	1,929	32,531	2,7154	19,518	2,2016	23,166	2,866	26,049	2,803
214	25,884	2,3198	27,533	4,088	30,714	3,9013	18,015	2,8537	20,107	2,482	18,716	1,567
217	20,178	1,647	Ghost				25,734	3,0676	Ghost			
219	21,322	2,571	26,048	4,0335	26,834	4,213	24,285	3,061	27,255	2,048	26,993	2,5859
220	17,076	3,535	Ghost				22,033	3,2015	Ghost			
221												
228	21,685	2,7774					26,938	1,927				
232	24,442	3,3536	42,041	5,0029	33,764	5,859	25,41	2,383	40,059	3,729	45,351	7,695
233	22,186	3,731	32,118	4,2014	32,144	5,454	26,254	3,274	32,347	2,87	34,68	3,23529
234	22,487	4,6334	38,697	3,0504	36,419	5,8337	21,257	3,56288	41,982	5,787	44,076	4,7512

Table 4.5: Calculated temperature using T1 temperature maps

The tables show the calculated temperature of the T1 weighted sequence. The scanning protocol included two T1 weighted measurements, one at the beginning of the scan and the second in the end of the scans. So it was possible to recognize the heating of the body throughout the scanning time.

No.	TPh1prä	TPh2prä	TPh1post	TPh2post	t Tod-MRT	T präScan	T postScan
133	12,6	24,2	23,5	23,6	24	21,7	20,4
201-09							
202-09					50 +/- 2	6,2	
205-09	7,6	22,6	19,3	20,5	~ 61	5,5	
206-09	8,7	20,5	21,4	21,7	64 +/- 2	4,6	
213-09	10,3	21,7	20,2	21,3	30 +/- 2	12,2	13,3
214-09	7,4	22,3	20,1	20,5	26	18,2	19,1
217-09	6,9	21,1	21,3	21,8	36	15,5	15
219-10	7,3	24	23,1	23,7	~ 12	23,7	24,7
220-10	6,9	23,2	20,8	21,2	40	11	12,1
221-10	8	23,4	19	19,4	53	6,3	10,1
228-10	7,2	22,5	23,1	23,2	18-19	21,6	21,3
232-10	5,2	21,9	22,4	23,1	28	15,2	16,3
233-10	9,8	22,3	23,5	23,5	29	17,9	16,9
234-10	7,1	23,1	21,9	22,7	50	11,2	13

Table 4.6: Summary table of the corpses' temperatures and post mortem delays

All manually measured temperatures were summarized in this lookup table. Comparing this table to the calculated table all temperatures differ. The T1 weighted sequence leads to a higher temperature and the diffusion sequence leads to a lower temperature. This proved that both methods are dependent on the effects of death.

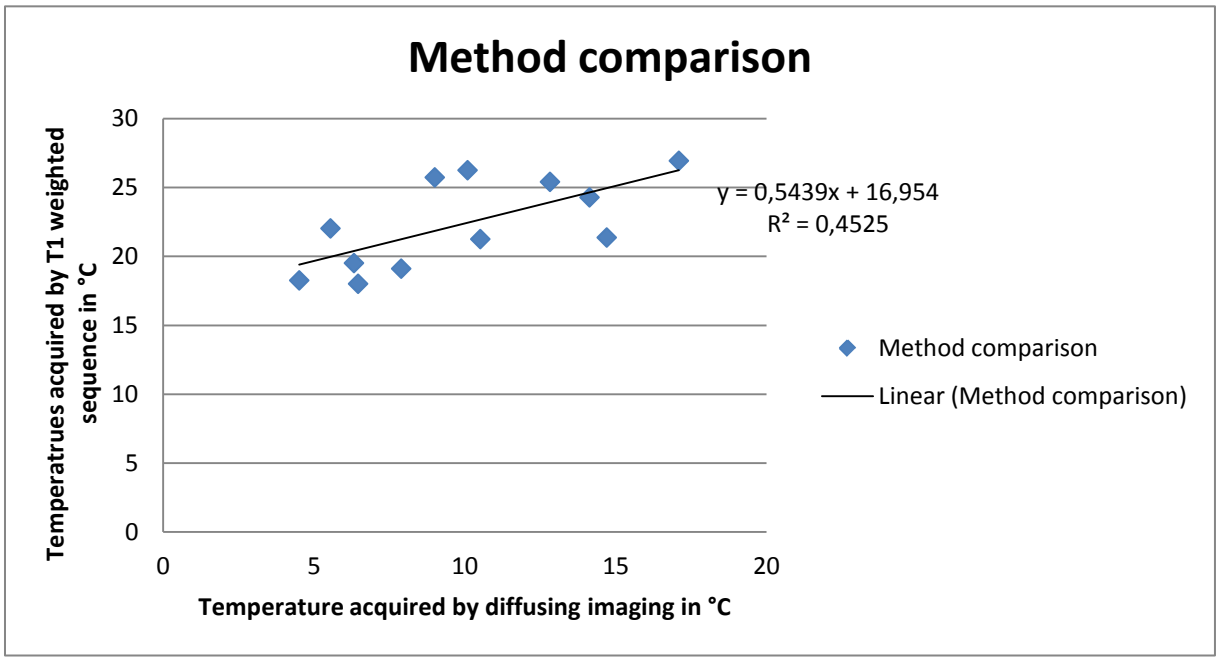

Figure 4.5: Method comparison between T1 and diffusion acquired data

The diagramm shows the scatterplot of the two different ways of acquiring the data. It is recogniseable that the difference of the temperature remains constant. The temperature effects both ways of acquiring data in a linear way.

4.3 Factorial variance analysis

Anova: factorial variance analysis MD und t-TOD-MRT

summary

groups	*quantity*	*sum*	*mean value*	*variance*
Diffusivity	14	0,0196004	0,001400029	2,89126E-08
time of death	14	521,5	37,25	258,4134615

ANOVA

	sum of sqares (SS)	*degrees of freedom (df)*	*mean sum of squares (MS)*	*focal (F)*	*P-value*	*critical F-Value*
differences between the groups	9712,207399	1	9712,207399	75,16796795	3,79016E-09	4,22520119
wihin the groups	3359,375	26	129,2067308			
sum	13071,5824	27				

Table 4.7: ANOVA of mean diffusivity and post mortem delay

The ANOVAs is a statistical method to find out how independent each variable is. In our case it was not possible to divide the effects of post mortem interval and temperature. One reason for this problem could have been the way how the corpses were stored. The longer the body is in the cooling room, the lower the temperature will be. This will lead to a dependence, which cannot be separated. Some data sets had an additional problem of a trauma. If there were any trauma, the liquor would be contaminated by blood. This blood could reduce the effect of diffusivity which leads to a cooler calculated temperature.

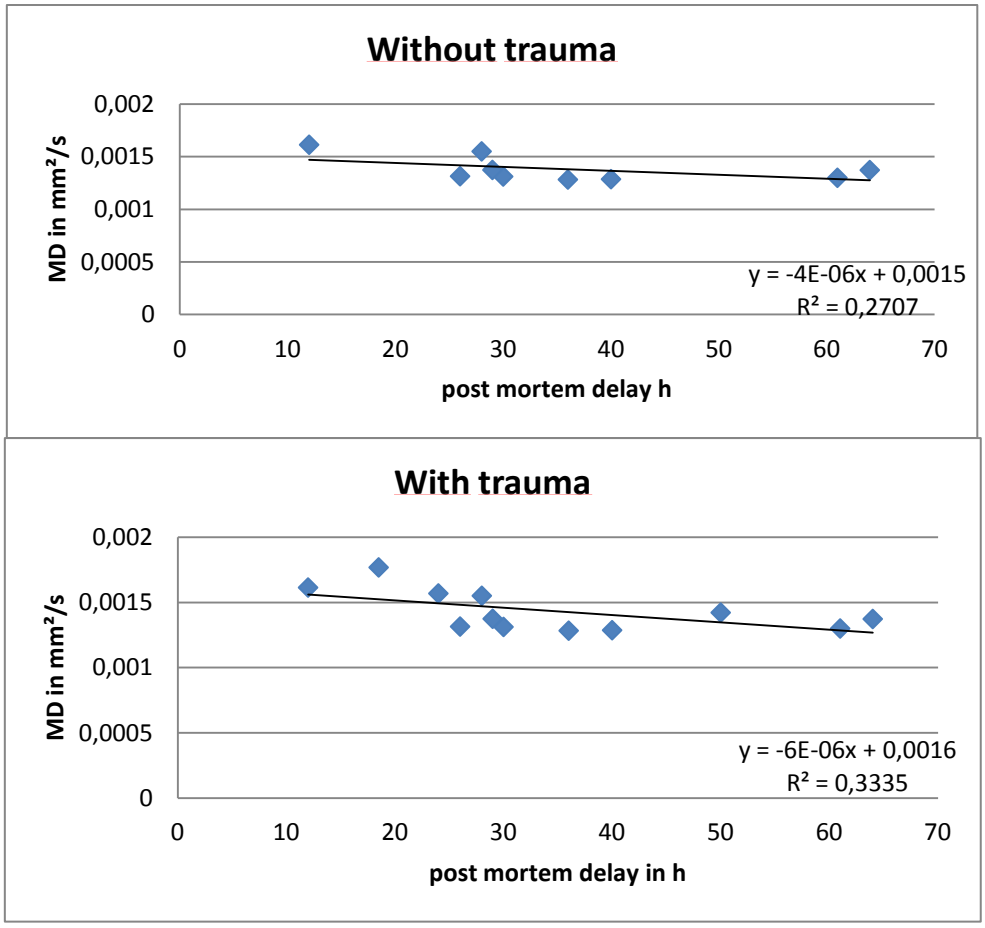

Figure 4.6: Comparison of trauma patients and non-trauma patients

In both diagrams the attenuation of the diffusivity was noticeable. It seemed that the trauma had no significant effect on the results.

4.4 Temperature correction

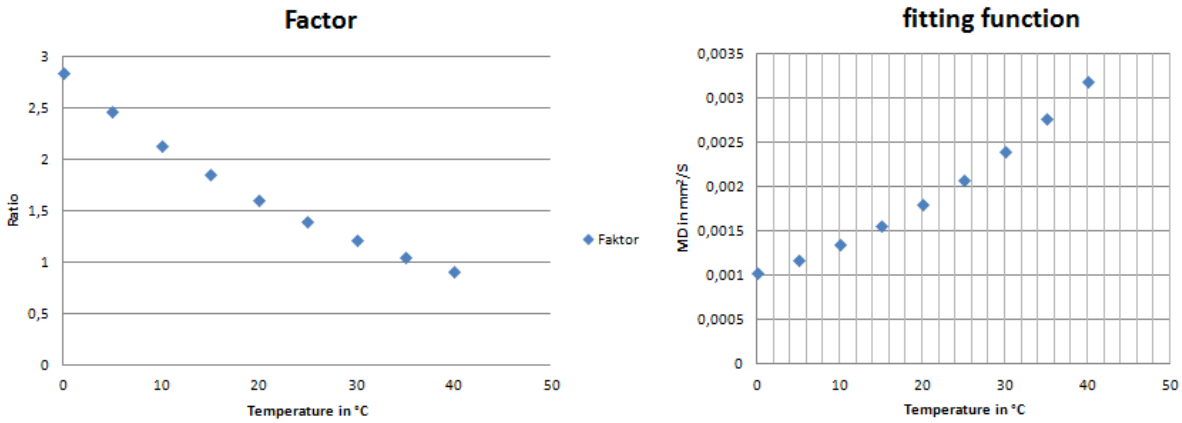

Figure 4.7: Temperature correction factor and fitting function

To correct the temperature error of the calculation the correction factor was introduced. With the knowledge of Simpson each self diffusion coefficient of water was known in the range from 0° C to 100 °C. Each factor was derived from the study of Simpson.

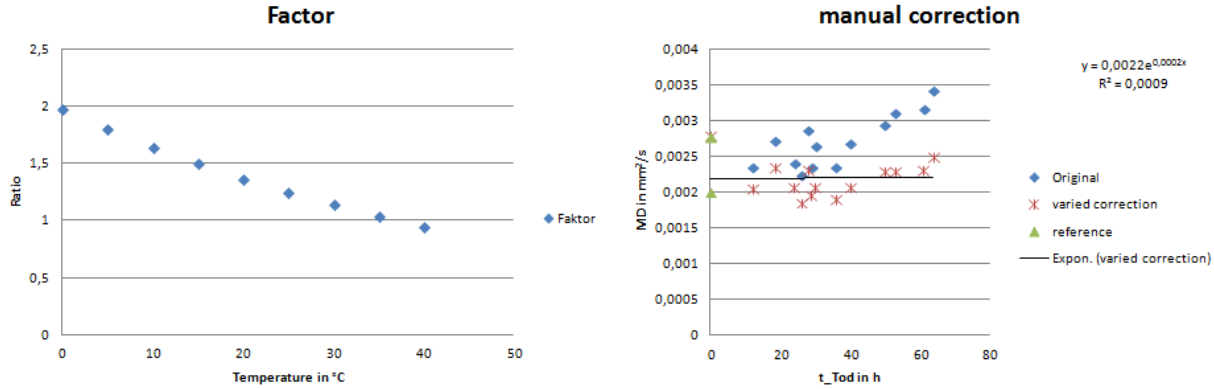

Figure 4.8: Manual correction

The blue symbols of the right diagram show the corrected data. It is noticeable, that the tendency of the mean diffusion values changed. The upper green symbol shows the diffusion coefficient of water and the lower symbol the diffusion coefficient of living people. Theoretically all data points have to be in one line because they had been corrected to 37 °C. These data points are corrected too much. Their diffusivity is about the diffusion coefficient of water. The left diagram shows the variation of the correction factor. The function of the factor was an exponential fitted function with a variable exponent. By adjusting the factor it was possible to turn the tendency of the corrected data into the right direction. This model can be used to assess of the temperature by knowing the diffusion coefficient of the liquor and the time of death.

4.5 Comparison of different b-values

All data sets before used a b-value of 2000 in the diffusion sequence. The next diagrams show the difference to a b-value of 1000.

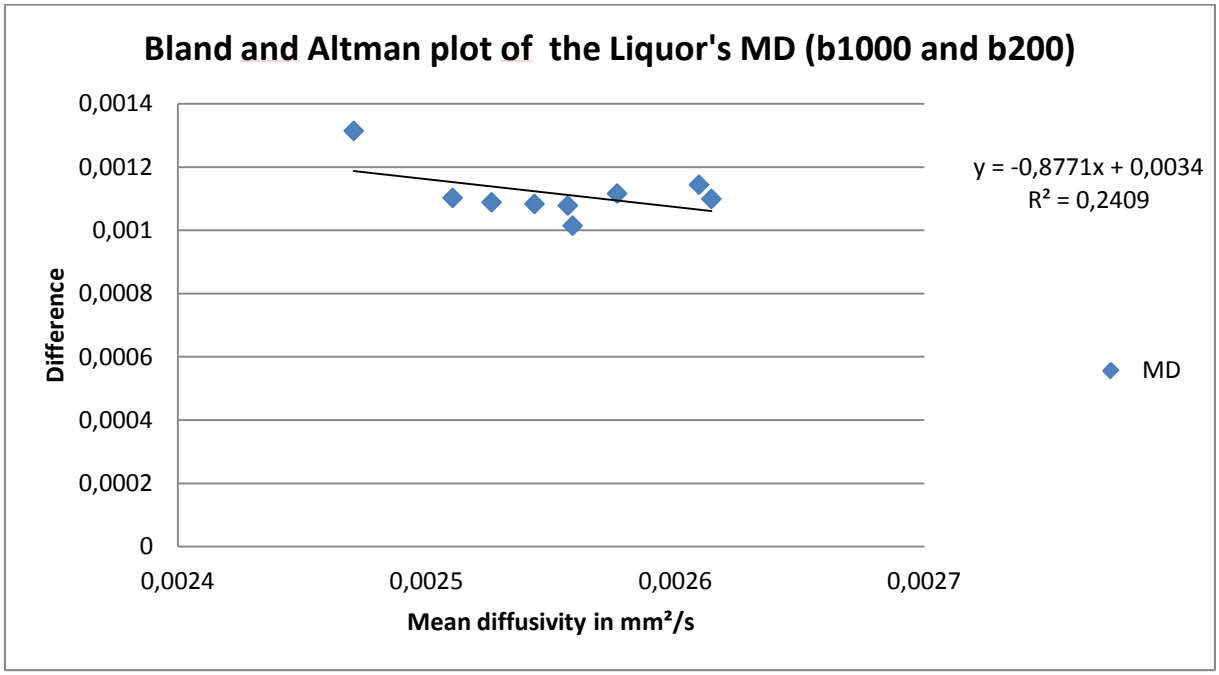

Figure 4.9: Bland and Altman plot of the Liquor's MD (b1000 and b200)

The Bland and Altman plot is a method for comparing two different methods of signal acquiring. The diagram shows that the difference between a b-value of 1000 and a b-value of 2000 remains constant. The measured values of the liquor cerebrospinalis with a diffusion sequence and a b-value of 2000 is constantly lower throughout whole region of diffusivity.

4.6 Diffusion coefficient in tissue

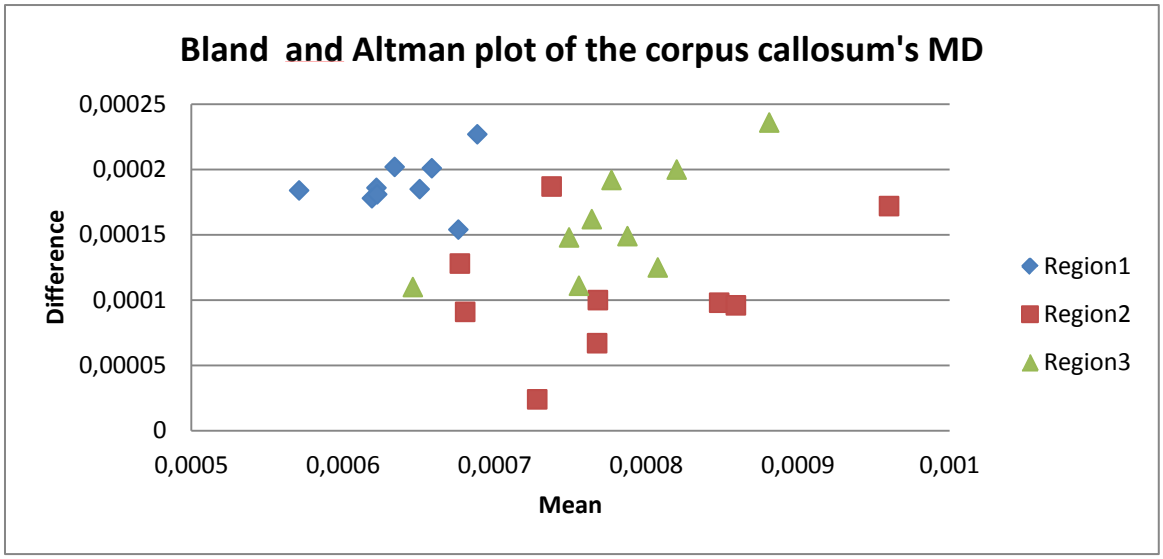

Figure 4.10: Bland and Altman plot of the corpus callosum's MD

The three regions were all taken from the corpus callosum. The regions themselves were clustered and were able to be separated.

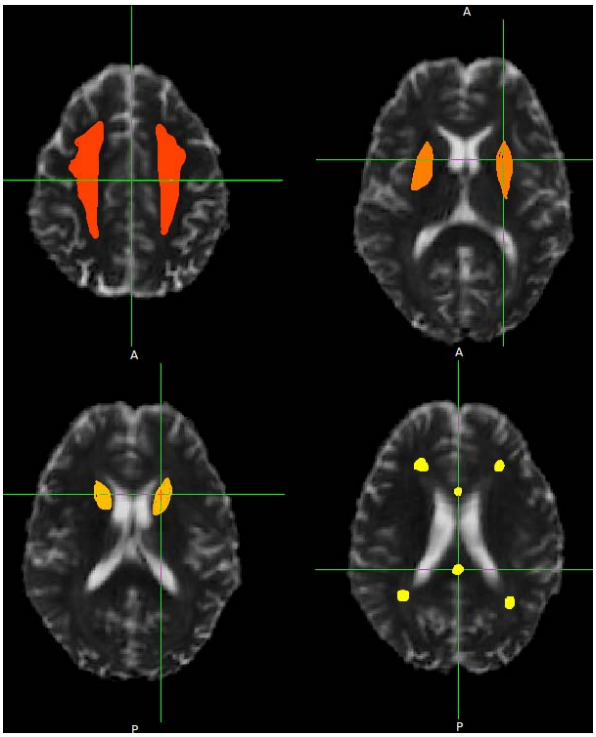

Figure 4.11: Region selection of the brains tissue

After analyzing the liquor cerebrospinalis, some different areas were chosen to see how the autolysis effects on tissue. Top left corner – centrum semioval, top right corner – Putamen, bottom left corner – Caput nuclei caudate and bottom right corner – white matter.

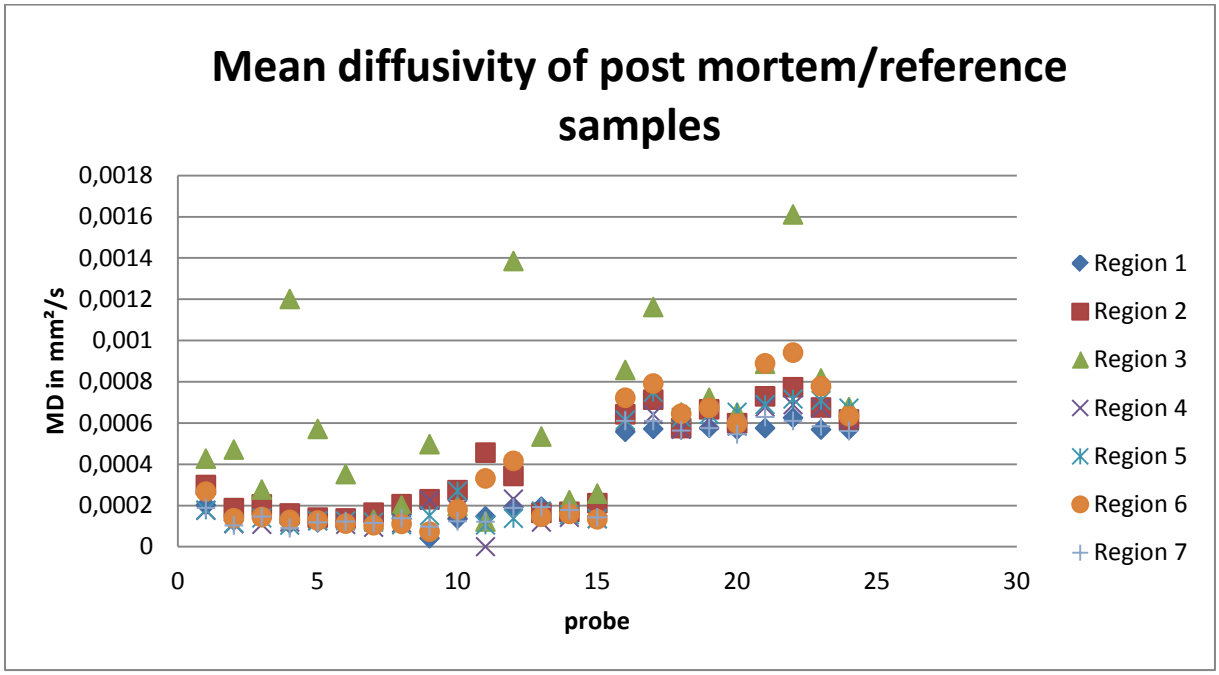

Figure 4.12: Mean diffusivity of post mortem/reference samples

4.7 Differences between tissue and cerebrospinal fluid

The diagram shows the differences in tissue between the corpses and reference group. All corpses show a lowered mean diffusivity.

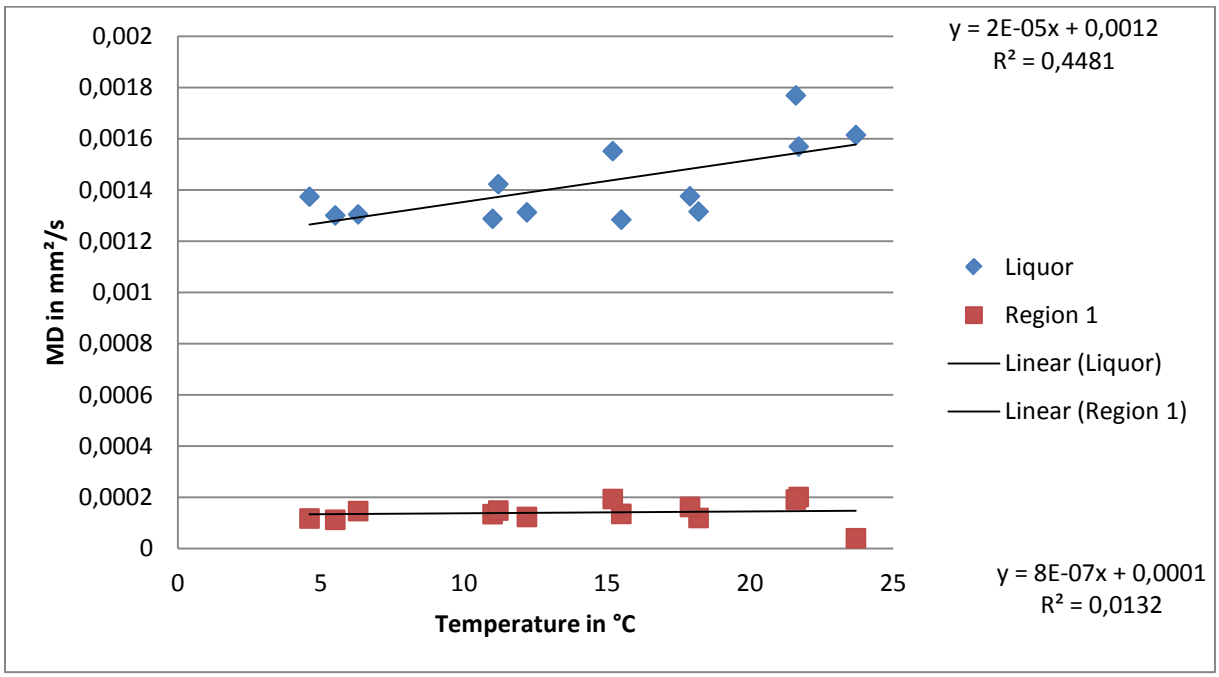

Figure 4.13: Comparison between the mean diffusivity of CSF and tissue depending on temperature

The mean diffusivity of tissue remained constant. The effect of temperature on tissues seems to be so small that the effect of restricted diffusion is dominated. On the other hand, the effect of temperature on Liquor was expected. The diffusion raised with increasing temperature. As we know from Simpson, the diffusion coefficient has to raise faster than our measured result. This was another important point which leads to the assumption that Liquor does not behave like water.

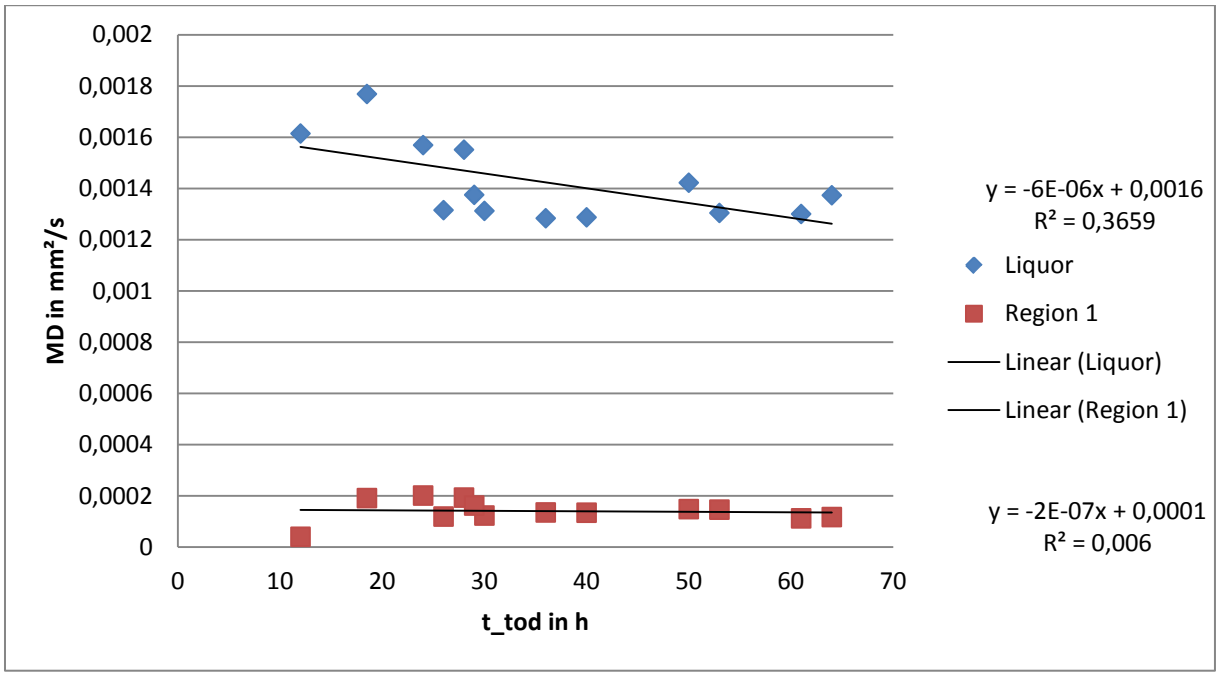

Figure 4.14: Comparison between the mean diffusivity of CSF and tissue depending on post-mortem delay

The relation between time of death and mean diffusivity was quite like the effect of temperature working on tissue. Contrary to the temperature of liquor the diffusivity of liquor was attenuated.

According to the information of our results, a different approach was tried to assess the temperature. All measured values indicated, that the Liquor does not behave like water after death.

4.8 Cell content in cerebrospinal fluid

As previously mentioned in the chapter methods, Wyler at al. had measured the cell content of the cerebrospinal fluid. The temperature of the corpses was also measured rectally.

Hospital collective 1 (20°C)			Hospital collective 2 (4°C)		
Case no.	Time after death	CSF cell count	Case no.	Time after death	CSF cell count
1	2.25	3	1	3	9
2	2.33	3	2	5.75	5
3	3	7	3	10.15	8
4	3	11	4	10.25	10
5	3.5	19	5	10.5	9
6	3.5	8	6	12.5	5
7	3.5	3	7	13	17
8	4	10	8	14.5	19
9	4.5	9	9	15.15	8
10	5	6	10	17.3	11
11	6.7	23	11	17.5	24
12	6.75	7	12	18	29
13	7	12	13	19.5	19
14	8.67	45	14	20	14
15	9	3	15	20.45	17
16	9	18	16	20.5	16
17	11	21	17	20.75	16
18	11.5	41	18	21.5	36
19	12.75	28	19	22	21
20	13	38	20	23	28
21	13.75	14	21	26.25	33
22	14.17	28	22	26.67	20
23	15.5	24	23	32.5	45
24	16	53	24	33.3	22
25	16	28	25	33.75	43
26	17	51	26	34.5	59
27	20.5	63	27	36.3	39
28	21	46	28	36.3	31
29	21.25	57	29	40	36
30	22	59	30	48	71
31	22	81	31	48.15	79
32	23	66	32	48.5	68
33	27.5	109	33	49.3	70
34	28.5	154	34	53.25	67
35	39	235			

Table 4.8: Hospital collective of cell count

The table was the result of his hospitality study. He performed the lumbar punctures on patients in the hospital for two years to get many corpses for a reliable result. The punctures were performed by the subarachnoid space at L2-3 or L3-4. The cells were counted in a counting chamber of 3 mm^3. The results had to be divided by the number three to get an absolute number of cell count. After collecting all cell counts, he formed the data in groups of five hour intervals and analyzed the significance of the groups. He found out, that the change of cell counts postmortem was so high that the formed groups were significantly different.

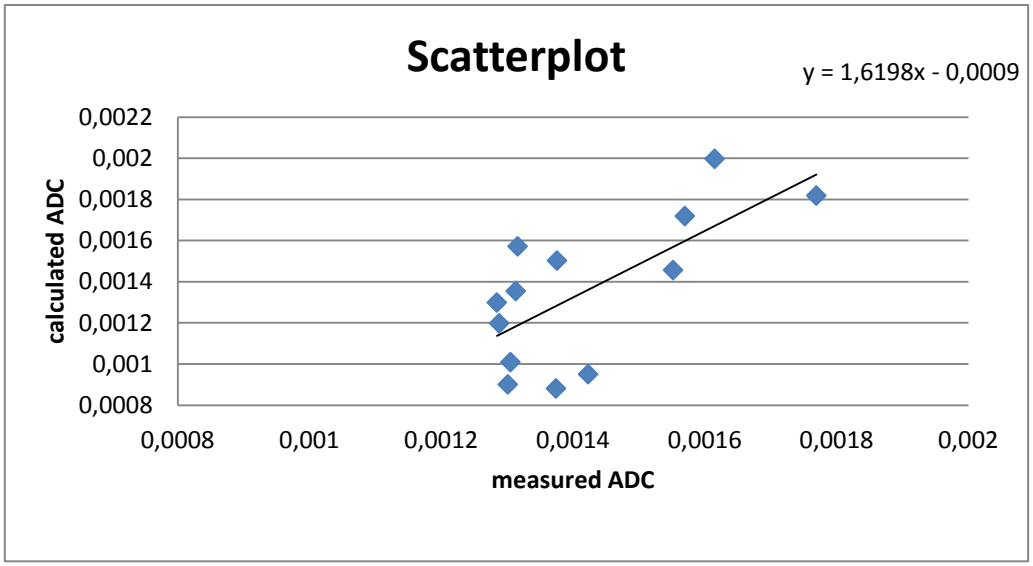

Figure 4.15: Scatterplot of the calculated and measured ADC

This scatter plot shows the comparison between the acquired and the calculated apparent diffusion coefficient. The gradient of the trend line can be adjusted by changing the gradient of the linear function. The paper of Takanori suggests the assumption that the gradient also depends on the cell size. The different amount of cells and cell types in Liquor, which get there after death, are responsible for the effect on the measured ADC. Adjusting the gradient of the cell denity vs. ADC plot by watching the scatter plot can simulate the effect of death. The angle in the scatter plot is 45°. This leads to the assumption that the cell density is corrected for the post mortem Liquor cell content.

5 Discussion

5.1 First model, the postmortem cerebrospinal fluid behaves like water

The first attempt of analyzing the effect of death was based on the hypotheses that the liquor behaves like water. This assumption might be true by healthy people but couldn't be realized in our study of cadaver. Tofts wrote in his paper that the diffusion coefficient of water can be used for thermometry. He mentioned that there might be a lower diffusion coefficient in the cerebrospinal fluid, but the effect is negligible. He also mentioned that the diffusion coefficient in vivo could be taken for noninvasive brain core thermometry. To make our results more comparable to the results of Tofts the dependencies of the diffusion coefficient have to be analyzed. Tofts took the calculated self diffusion coefficients from the paper of Mills , whereas we took the measured self diffusion coefficients of Simpson.

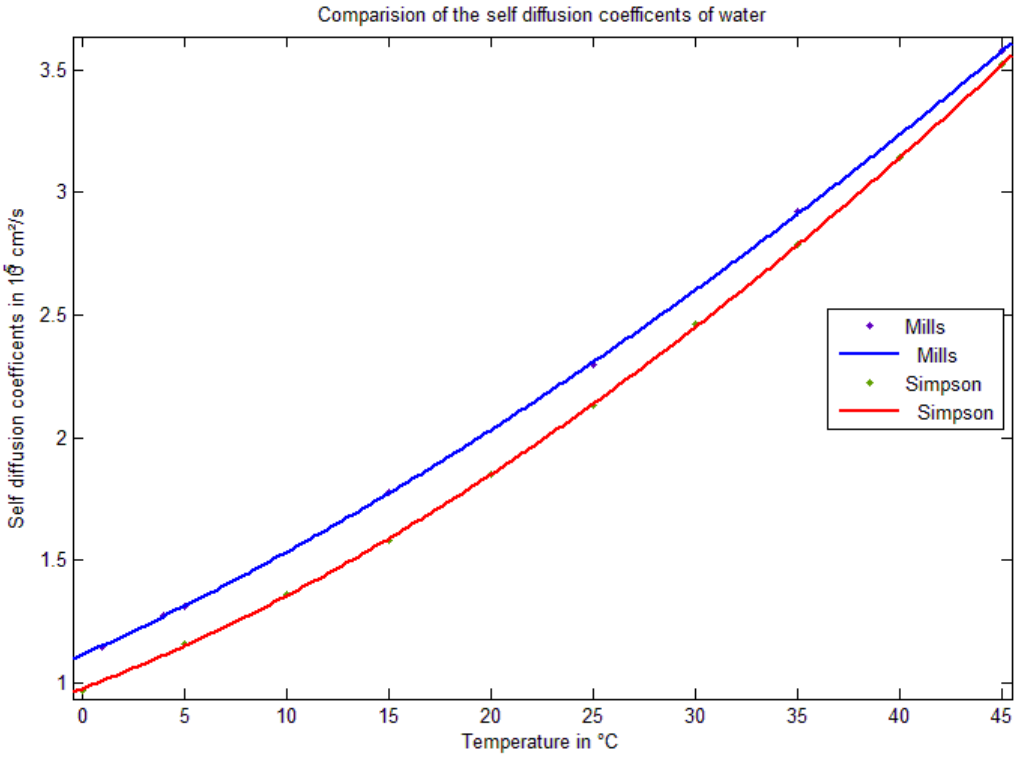

Figure 5.1: Comparison of the self diffusion coeffiecents of water

The figure shows the slight differences between the self diffusion coefficients of water. Both data sets were figured by a cubic function. It is noticeable that the function, generated out of the measured values of Simpson, remains lower throughout the whole range of temperature. This will cause a higher temperature for the same diffusivity by using them. Especially the

temperature range within the focus of the post mortem samples will affect a greater difference.

The measurement of the reference group was much more problematic as expected. The pulsation and the partial volume effects of the liquor and the bordered on tissue affect the diffusivity too much. LR Kozak et al. [13]Showed how complicated it is to measure the temperature in vivo. He tried to get rid of the pulsation artifacts by taking just the diffusion vectors of the direction which pointed along the bending of the lateral ventricle. After the reduction of the directions of diffusion to nine and excluding the outliers (he implemented two different thresholds. All temperatures lower than 30 °C and higher than 55°C were ignored) he got physiologically meaningful results. Tofts wrote that an in vivo measurement seems to be reliable without those corrections, which is disproved by the paper of Kozak. He also wrote that one of the three cadavers he had measured was in the refrigerator for a long time by an unreliable control of temperature. He estimated a brain core temperature of this cadaver of 1.0 °C. The duration of refrigeration of this body was about 48 hours. The other two cadavers were cooled for 14 and 18 hours. The estimation for these bodies was 9.7 °C and 9.9 °C. Regarding his assumption that there is no effect of death which could affect the diffusivity in liquor he assessed he wrote that these were reliably temperature values. After 1.5 hours he measured the temperature again which results a calculated temperature of 12 °C. A manual probe of the third cadaver was also taken. The results of the manually taken temperature were 11 °C before imaging and 16 °C after two hours. There is no explanation why the temperature differs so much two hours after the manually taken measurement.

The results of our measurements show similar effects. The longer the corpses remain in the cooling chamber the lower the diffusion coefficient will be. Additional to this effect a postmortem effect will lower the diffusion coefficient. This might explain why the temperature of the manually taken probes of Tofts differs from the assessed. The effect of death is stronger than the temperature effect. The relation between post mortem delay and diffusion in our results shows that the effect of attenuating diffusion still happens after 50 hours of death. The corpses already reached a steady state of the temperature (the corpse has the same temperature as the cooling chamber) and the diffusion coefficient still falls. By assuming that the cerebrospinal fluid behaves like water, a chemical change of the liquor could be the reason.

J. I Coe [14] describes the postmortem chemistry of the body and their practical considerations. For the cerebrospinal fluid following information were found:

Carbohydrates:

Glucose: The postmortem glycolysis still occurs, i. e. lucose level will fall after death.
Lactic Acid: The lactic acid will rise after death, especially in the tenth hour after death

Nitrogenous Compounds:

Urea: The urea concentratin remains constant within the first 36 h postmortem
Nonprotein Nitrogen: During the first 30 hours the nonprotein Nitrogen will increase.
Creatinin:The creatinin level also remains constant.
Creatin: Creatin will rise in contrast to creatinin.
Amino: Acid Nitrogen: Amino acid nitrogen will rise due to enzymatic breakdown of proteins.
Ammonia: A linear rise of ammonia was recognized with increasing time of death.
Uric Acid and Xanthine: Both components will rise after death.

Electorlytes:

Na, Cl and Ca concentration will be less after death, whereas K, HCO_3 and Mg will rise.

Many of those components of the cerebrospinal fluid depend on illnesses before death. The exact influences of each component to the diffusion constant are not known. Tofts wrote that an increase of viscosity due to dissolved proteins was responsible for the attenuation of diffusivity, but he ignored this result in his model.

5.2 Diffusion coefficient of tissue:

It is noticeable that tissue behaves completely different. The values of the measured diffusion coefficients of the centrum semioval remain constant over the post mortem delay and temperature. The effect of autolysis does not influence the tissues diffusivity as much as the liquor is influenced. The restricted diffusion within the cells is the dominated effect. This information can be used for post mortem fiber tracking. It is still possible to reconstruct the nervous cells after death. A noninvasive autopsy could still be used to detect illnesses of the nervous system such as amyotrophic lateral sclerosis. The results of the reference groups were analogical to the postmortem results. All diffusion coefficients of the different postmortem cases seem to be similar. The reference group shows the same result with a higher average level of diffusivity. The big difference of temperature is responsible for the extenuated restricted diffusion within the cells.

5.3 Second model, cell count in the cerebrospinal fluid increases after death

All previous assumptions neglect the existence of cells in the cerebrospinal fluid Tofts mentioned an appearance of debris in his research, but he assumed that they settle to the bottom of the ventricle. Itabashi et al. [15] reviewed the cell content in postmortem cerebrospinal fluid. He divided the different cells into two categories – cases without central nervous system pathology and cases with accidentally introduced cells from the tissue.

Cell types which were found without CNS pathology:

- Lymphocytes
- Pia-arachnoidal cells
- Ependymal cells
- Choroid plexus epithelium

Cell types introduced by trauma:

- Epidermal squamous cells
- Capillaries
- Erythrocytes
- Adipose tissue
- Fibrous tissue
- Skeletal muscle cells
- Nerve cells
- Glia

Nerve cells and glia were introduced from the underlying structures and the other trauma introduced cells were from the overlying tissue.

Wyler et al. analyzed the amount and types of cells in the cerebrospinal fluid after death. The amount of cells in the liquor depends on the time of death. The information about the cell content is the base of our model. In the first few hours after death an active transport of the cells into the cerebrospinal fluid takes place, later only passive transport occurs. The identification of the cells is quite difficult. Platt et al. [16] investigated the pleocytosis in post mortem liquor. He showed that is impossible to identify the cells after 12 hours of death. The cells became vacuolated and no histochemical identification could be done. Wyler additional tried to identify the cells in CSF by electron microscopy, but the data wasn't shown in his paper. By using a microscope to evaluate the cells he also came to the conclusion, that the cytoplasm of the cells were swollen and vacuolated. They assumed, the effect occurs in relation to the time of death. The cells will swell for three to four days before they burst.

Takanori et al. describes the effect of cell density and apparent diffusion coefficient. His phantoms contain Ramos cells with a diameter of 11.6 µm. The whole measurement was carried out with a temperature of 37°C. The information of the destroyed sonicated cells and the normal Ramos cells leads to following assumption. The bigger the cells are, the faster the diffusion coefficient will attenuate relating to the cell density. This effect might be the reason for the lowered diffusion coefficient in the liquor. After few hours of death more and more cells contaminate the CSF. The self diffusion of water in the extracellular CSF will be restricted by the amount of cells. Additionally to this effect, the cells will swell and need additional water from the CSF. Additional swelling can occur by inflammation of tissue. The cells which were introduced are not known. With the information of cell types, which were listed before (cells found without CNS pathology), compared to the size of the Ramos cells leads to the assumption that nearly all cells are much bigger. This occurs to a faster dependency of ADC to the cell density. With the aspect of swollen cells, it will become the major effect of attenuation.

A smaller effect which influences the diffusivity is the pH-Value. The pH value of CSF is normally 7.32 to 7.36. Postmortem the pH-value will decrease. After a few hours the pH-value will come to a steady state. The pH-value of the CSF is alsow influenced by illnesses. Long term diseases and the agonal state are the factors which mainly influence the falling pH-Value. Altsheimer disease for example will lower the pH-value to 6.5.

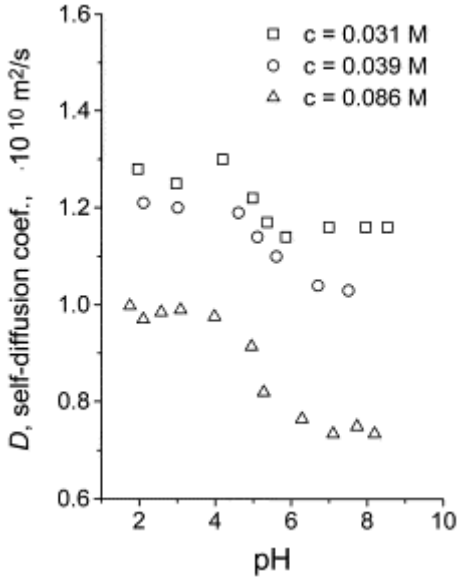

Figure 5.2: Diffusion dependency on pH-value

The figure was taken from the paper "self-diffusion and self-association of lysozome molecules in solution" written by Nesmelova [17]*. It shows the dependency of self diffusion on the pH-value by different concentrations of lysozomes. The assumption, that the change on pH-value will affect the diffusion coefficient cannot be totally excluded.*

6 Conclusion

Diffusion weithed imaging can be used as a method for temperature assessment within an aqueous solution. In vivo and postmortem assessment of the bodies' temperature is not as simple as it was described by Tofts [5]. The assumption that the diffusivity of water can be used for assessing the temperate of the cerebrospinal fluid cannot be confirmed. In vivo, the pulsation of the cerebrospinal fluids within the brains ventricle leads to great variations of the assessed temperature. Even with methods which were used by LR Kozak et [13]. al. a correct assessment is not possible without knowing the composition of cerebrospinal fluid. The temperature assessment within the corpses is also not as simple as mentioned by Tofts. The observations of the cerebrospinal fluids' diffusivity showed a lower assessment of the temperature as the manually taken rectal temperature. The cell content and the autolysis effect on the viscosity of the cerebrospinal fluid lead to wrong assessment. The temperature correction of the first applied model, which was based on the assumption that the CSF behaves like water, showed an overcorrection of all datasets. A manually carried out correction might compensate this overcorrection but this will be not a reliable method. An attempt to separate the effects of postmortem delay and temperature failed regarding to the storage in the cooling chamber. The cooling of the corpses is associated to the postmortem time which leads to this inseparability. The second model includes the information of the cell content. It can be shown that an assessment of the apparent diffusion coefficient of water within the post mortal cerebrospinal fluid can be done if you know the time of death and temperature. The results of our assessment showed an approach to the measured data. The used information of the Ramos cells are not reliable for the assessment but showed a possible prediction of the ADC. Anyway more information about the exact cell content is needed to predict a reliable result.

7 Bibliography

[1] U. Göttingen, "Universitätsmedizin Göttingen," 2013. [Online]. Available: http://www.mrforschung.med.uni-goettingen.de/dwi_dti.htm. [Accessed February 2013].

[2] P. S. Tofts, J. S. Jackson, D. J. Tozer, M. Cercignani, G. Keir, D. G. MacManus, G. R. Ridgway, B. H. Ridha, K. Schmierer, D. Siddique, J. S. Thornton, S. J. Wroe and N. C. Fox, "Imaging Cadaver: Cold FLAIR and Noninvasive Brain Thermotmetry Using CSF Diffusion," *Magnetic Resonance in Medicine,* pp. 59:190-195, 2008.

[3] D. Le Bihan, E. Breton, D. Lallemand, M.-L. Aubin, J. Vignaud and M. Laval-Jeantet, "Seperation of diffusion and perfusion in intravoxel incoherent motion mr imaging," *Radiology,* pp. 168:497-505, 1988.

[4] R. Stollberger, *Bioimaging Scriptum,* TUGraz, 2009.

[5] P. Tofts, Quantitativ MRI of the Brain - Measuring changes caused by disease, England: John Wiley & Sons, Ltd, 2003.

[6] V. Rieke and K. B. Pauly, "MR Thermometry," *Journal of Magnetic Resonance Imaging,* pp. 27:376-390, 2008.

[7] R. Mills, "Self-Diffusion in Normal and Heavy Water in the Range 1-45°," *The Journal of Physicak Chemistry,* pp. 77:685-688, 1973.

[8] "Oxford Centre for Functional MRI of the Brain," [Online]. Available: http://fsl.fmrib.ox.ac.uk/fsl/fslwiki/EDDY. [Accessed January 2013].

[9] "Oxford Centre for Functional MRI of the Brain," [Online]. Available: http://fsl.fmrib.ox.ac.uk/fsl/fslwiki/TBSS. [Accessed January 2013].

[10] D. Wyler, W. Marty and W. Bär, "Correlation between the post-mortem cell content of cerebrospinal fluid and time of death," *International Journal of Legal Medicine,* pp. 106;194-199, 1994.

[11] T. Sasaki, M. Kuroda, K. Katashima, M. Ashida, H. Matsuzaki, J. Asaumi, J. Murakami, S. Ohno, H. Kato and S. Kanazawa, "In Vitro Assessment of Factors Affecting the Apparent Diffusion Coefficent of Ramos Celss Using Bio-phantoms," *Acta Medica Okayama,* pp. 66:263-270, 2012.

[12] J. H. Simpson and H. Y. Carr, "Diffusion and Nuclear Spin Relaxation in Water," *The Physical Review,* pp. 11:1201-1202, 1958.

[13] L. Kozak, M. Bango, M. Szabo, G. Rudas, Z. Vidnyansky and Z. Nagy, "Using diffusion MRI for measuring the temperature of Cerebrospinal fluid within the lateral ventricles," *Acta Paedatrica,* pp. 99:237-243, 2010.

[14] J. I. Coe, "Postmortem Chemistry: Practical Considerations and a Review of the Literature," *Journal of Forensic Science,* pp. 19:18-32, 1974.

[15] H. H. Itabashi, J. M. Andrews, U. Tomiyasu, S. S. Erlich and L. Sathyavagiswaran, Forensic Neuropathologie - A Practical Review of the Fundamentals.

[16] M. Platt, S. McClure, R. Clarke, W. Spitz and W. Cox, "Postmortem cerebrospinal fluid pleocytosis," *International Journal of Legal Medicine,* pp. 106:194-199, 1994.

[17] I. V. Nesmelova and V. D. Fedotov, "Self-diffusion and self-association of lysozyme molecules in solution," *Biochimica et Biophysica Acta (BBA) - Protein Structure and Molecular Enzymology,* pp. 1383:311-316, 1998.

8 List of figures

9 List of tables

EIDESSTATTLICHE ERKLÄRUNG

Ich erkläre an Eides statt, dass ich die vorliegende Arbeit selbstständig verfasst, andere als die angegebenen Quellen/Hilfsmittel nicht benutzt und die den benutzten Quellen wörtlich und inhaltlich entnommenen Stellen als solche kenntlich gemacht habe.

Graz, am ……. ……..

(Unterschrift)

Englische Fassung:

STATUTORY DECLARATION

I declare that I have authored this thesis independently, that I have not used other than the declared sources / resources and that I have explicitly marked all material which has been quoted either literally or by content from the used sources.

……. ……..

date (signature)